The systematics of the Mongolepidida (Chondrichthyes) and the Ordovician origins of the clade

Plamen Andreev, Michael I Coates, Valentina Karatajūtė-Talimaa, Richard M Shelton, Paul R Cooper, Nian-Zhong Wang, Ivan J Sansom

The Mongolepidida is an Order of putative early chondrichthyan fish, originally erected to unite taxa from the Lower Silurian of Mongolia. The present study reassesses mongolepid systematics through the examination of the developmental, histological and morphological characteristics of scale-based specimens from the Upper Ordovician Harding Sandstone (Colorado, USA) and the Upper Llandovery–Lower Wenlock Yimugantawu (Tarim Basin, China), Xiushan (Guizhou Province, China) and Chargat (north-western Mongolia) Formations. The inclusion of the Mongolepidida within the Class Chondrichthyes is supported on the basis of a suite of scale attributes (areal odontode deposition, linear odontocomplex structure and lack of enamel, cancellous bone and hard-tissue resorption) shared with traditionally recognized chondrichthyans (euchondrichthyans, e.g. ctenacanthiforms). The mongolepid dermal skeleton exhibits a rare type of atubular dentine (lamellin) that is regarded as one of the diagnostic features of the Order within crown gnathostomes. The previously erected Mongolepididae and Shiqianolepidae families are revised, differentiated by scale-base histology and expanded to include the genera *Rongolepis* and *Xinjiangichthys*, respectively. A newly described mongolepid species (*Solinalepis levis* gen. et sp. nov.) from the Ordovician of North America is treated as family *incertae sedis*, as it possesses a type of basal bone tissue (acellular and vascular) that has yet to be documented in other mongolepids. This study extends the stratigraphic and palaeogeographic range of Mongolepidida and adds further evidence for an early diversification of the Chondrichthyes in the Ordovician Period, 50 million years prior to the first recorded appearance of euchondrichthyan teeth in the Lower Devonian.

1 The systematics of the Mongolepidida (Chondrichthyes)

2 and the Ordovician origins of the clade

5 Plamen S. Andreev[1], Michael I. Coates[2], Valentina Karatajūtė-Talimaa[3], Richard M.

6 Shelton[4], Paul R. Cooper[4], Nian-Zhong Wang[5†] and Ivan J. Sansom[1]

8 [1]School of Geography, Earth and Environmental Sciences, University of Birmingham,

9 Edgbaston, Birmingham B15 2TT, UK

10 [2]Department of Organismal Biology and Anatomy, University of Chicago, Chicago, Illinois

11 60637-1508, USA

12 [3]Department of Geology and Mineralogy, Vilnius University, M.K. Ciurlionio 21/27, LT-03101

13 Vilnius, Lithuania

14 [4]School of Dentistry, College of Medical and Dental Sciences, University of Birmingham, St

15 Chad's Queensway, Birmingham B4 6NN, UK

16 [5]Laboratory of Evolutionary Systematics of Vertebrates, Institute of Vertebrate Palaeontology

17 and Palaeoanthropology, Chinese Academy of Sciences, PO Box 643, Beijing 100044, China;

18 deceased

19 Corresponding authors

20   Plamen Andreev, p.andreev@bham.ac.uk

21   Ivan Sansom, i.j.sansom@bham.ac.uk

22   ABSTRACT

23   The Mongolepidida is an Order of putative early chondrichthyan fish, originally erected

24   to unite taxa from the Lower Silurian of Mongolia. The present study reassesses

25   mongolepid systematics through the examination of the developmental, histological

26   and morphological characteristics of scale-based specimens from the Upper

27   Ordovician Harding Sandstone (Colorado, USA) and the Upper Llandovery–Lower

28   Wenlock Yimugantawu (Tarim Basin, China), Xiushan (Guizhou Province, China) and

29   Chargat (north-western Mongolia) Formations.

30   The inclusion of the Mongolepidida within the Class Chondrichthyes is supported on

31   the basis of a suite of scale attributes (areal odontode deposition, linear

32   odontocomplex structure and lack of enamel, cancellous bone and hard-tissue

33   resorption) shared with traditionally recognized chondrichthyans (euchondrichthyans,

34   e.g. ctenacanthiforms). The mongolepid dermal skeleton exhibits a rare type of

35   atubular dentine (lamellin) that is regarded as one of the diagnostic features of the

36   Order within crown gnathostomes.

37   The previously erected Mongolepididae and Shiqianolepidae families are revised,

38   differentiated by scale-base histology and expanded to include the genera *Rongolepis*

39   and *Xinjiangichthys*, respectively. A newly described mongolepid species (*Solinalepis*

40   *levis* gen. et sp. nov.) from the Ordovician of North America is treated as family

41   *incertae sedis*, as it possesses a type of basal bone tissue (acellular and vascular)

42   that has yet to be documented in other mongolepids.

43   This study extends the stratigraphic and palaeogeographic range of Mongolepidida

44   and adds further evidence for an early diversification of the Chondrichthyes in the

45   Ordovician Period, 50 million years prior to the first recorded appearance of

46   euchondrichthyan teeth in the Lower Devonian.

60   **Keywords** Mongolepids, *Solinalepis* gen. nov., Palaeozoic, Scales, Morphogenesis,

61   Odontocomplex

INTRODUCTION

64   Middle Ordovician to upper Silurian strata have yielded a number of isolated scale

65   remains that have been assigned to the chondrichthyans with varying degrees of

66   confidence. This 50 million year record pre-dates the first appearance of teeth and

67   articulated skeletons (*Leonodus* and *Celtiberina* Botella et al., 2009; *Doliodus* Miller,

68   Cloutier & Turner, 2003; Maisey, Miller & Turner, 2009 and *Antarctilamna* Young,

69   1982) of traditionally recognized chondrichthyans (euchondrichthyans *sensu* Pradel et

70   al, 2014), as well as body fossils of acanthodian-grade stem chondrichthyans

71   (Brazeau & Friedman, 2015 and references therein). These, largely microscopic,

72   remains include the elegestolepids (Karatajūtė-Talimaa, 1973; Žigaitė & Karatajūtė-

73   Talimaa, 2008; Andreev et al., in press), sinacanthids (Zhu, 1998; Sansom, Wang &

74   Smith, 2005), taxa such as *Tezakia* and *Canyonlepis* from the Ordovician of North

75   America (Sansom, Smith & Smith, 1996; Andreev et al., 2015), *Tantalepis* (Sansom et

76   al., 2012), *Kannathalepis* (Märss & Gagnier, 2001) and *Pilolepis* (Thorsteinsson,

77   1973), and, perhaps the most widely distributed and diverse collection of what Ørvig

78   and Bendix-Almgreen, quoted in Karatajūtė-Talimaa (1995), referred to as

79 'praechondrichthyes', the mongolepids (Karatajūtė-Talimaa et al., 1990; Karatajūtė-

80 Talimaa & Predtechneskyj, 1995; Sansom, Aldridge & Smith, 2000). It is the latter

81 which this work concentrates on, re-assessing and re-defining previously described

82 members of the Mongolepidida, and describing a new taxon that extends the range of

83 the Order into the Ordovician, adding further evidence for a diversification of early

84 chondrichthyans as part of the Great Ordovician Biodiversification Event that

85 encompasses a wide variety of taxa, both invertebrate (e.g. Webby, Paris & Droser,

86 2004; Servais et al., 2010) and vertebrate (Sansom, Smith & Smith, 2001; Turner,

87 Blieck & Nowlan, 2004).

Previous work on mongolepids

89 Mongolepids were first described by Karatajūtė-Talimaa et al. (1990) and Karatajūtė-

90 Talimaa (1995) from the Chargat Formation (Upper Llandovery–Lower Wenlock) in

91 north-western Mongolia, together with a diverse assemblage of early vertebrates

92 including pteraspidomorphs (Karatajūtė-Talimaa, unpublished data), thelodonts

93 (Žigaitė, 2004, 2013; Žigaitė, Karatajūtė-Talimaa & Blieck, 2011), acanthodians

94 (Karatajūtė-Talimaa & Smith, 2003) and elegestolepids. The first erected species,

95 *Mongolepis rozmanae*, was subsequently added to with the description of *Teslepis*

96 *jucunda* Karatajūtė-Talimaa & Novitskaya (1992) and *Sodolepis lucens* Karatajūtė-

97 Talimaa & Novitskaya (1997), also from the Chargat Formation. Recently the

98 stratigraphic ranges of *Mongolepis* and *Teslepis* have been extended to include

99 Aeronian (Middle Llandovery) and Sheinwoodian (Lower Wenlock) sedimentary

100 sequences from Altai and Tuva (Sennikov et al., 2015). *Shiqianolepis hollandi* from the

101 Xiushan Formation (Telychian) of south China was also placed within the Order by

102 Sansom, Aldridge & Smith (2000), although a new Family, the Shiqianolepidae, was

103 erected based upon an interpretation of the scale growth patterns within mongolepids.

104 Additional material from the upper Llandovery of the Tarim Basin (Xinjiang Uygyr

105 Autonomous Region, north-west China) is also referable to the group (unpublished

106 data). Thus, to date, the distribution of mongolepids has been limited to a very narrow

107 time frame (Llandovery–Wenlock) and is concentrated within the Mongol-Tuva, Altai,

108 South China and Tarim tectonic blocks. The taxonomic placement of the group has

109 been greatly hampered by the absence of articulated specimens that exhibit any

110 anatomical detail of the mongolepid bodyplan (Karatajūtė-Talimaa et al., 1990;

111 Karatajūtė-Talimaa, 1995).

112

MATERIALS AND METHODS

113 MATERIALS AND METHODS

114 All examined material consists of isolated scales extracted by petroleum ether or

115 acetic acid disaggregation of rock samples from the Sandbian Harding Sandstone of

116 central Colorado, USA, the Upper Llandovery–Lower Wenlock Chargat Formation of

117 north-western Mongolia, the lower and upper members of the Telychian Yimugantawu

118 Formation of Xinjiang (Tarim Basin, China) and the lower Member of the Telychian

119 Xiushan Formation (Guizhou Province, China).

120   Scale morphology was documented using the JEOL JSM-6060 and Zeiss EVO

121 LS scanning electron microscopes at the School of Dentistry of the University of

122   Birmingham, UK. Prior to imaging specimens were sputter-coated with gold/palladium

123   alloy.

124   For the purpose of studying scale histology and internal structure, doubly

125   polished thin sections of scales were examined with Nomarski differential interference

126   contrast microscopy (using a 'Zeiss Axioskop Pol' polarization microscope) and

127   scanning electron microscopy (using a JEOL JSM-6060 SEM at the School of

128   Dentistry, University of Birmingham, UK).

129   Scale examination with X-ray radiation was performed with the SkyScan 1172

130   microtomography scanner at the School of Dentistry, University of Birmingham, UK.

131   The acquired microradiographs (tomographic projections) were taken at 0.3° intervals

132   over a 180° rotation cycle at exposure times of 400 ms, using a 0.5 mm thick X-ray

133   attenuating Al filter. These image data were processed with the SkyScan NRecon

134   reconstruction software for the purpose of generating sets of microtomograms that

135   were converted into volume renderings in Amira 5.4 3D analysis software.

136   Figured specimens are housed in the Lapworth Museum of Geology, University

137   of Birmingham, UK (BU prefix), the Nanjing Institute of Geology and Palaeontology,

138   Chinese Academy of Sciences, Nanjing, China (NIGP prefix) and the Institute of

139   Vertebrate Paleontology and Paleoanthropology, Chinese Academy of Sciences,

140   Beijing, China (IVPP V prefix). The examined non-figured scales have not been given

141   collection numbers. Additional mongolepid material, alluded to but not described in this

142   work (referred to as unpublished data above), from the Tarim Basin of China is housed

143 in and registered at the Institute of Vertebrate Paleontology and Paleoanthropology,

144 Chinese Academy of Sciences.

145 The electronic version of this article in Portable Document Format (PDF) will represent a

146 published work according to the International Commission on Zoological Nomenclature

147 (ICZN), and hence the new names contained in the electronic version are effectively

148 published under that Code from the electronic edition alone. This published work and

149 the nomenclatural acts it contains have been registered in ZooBank, the online

150 registration system for the ICZN. The ZooBank LSIDs (Life Science Identifiers) can be

151 resolved and the associated information viewed through any standard web browser by

152 appending the LSID to the prefix http://zoobank.org/. The LSID for this publication is:

153 urn:lsid:zoobank.org:pub:3C24AE11-1F12-4B16-B04D-480CA204CCEA. The online

154 version of this work is archived and available from the following digital repositories:

155 PeerJ, PubMed Central and CLOCKSS.

156

157 **Definitions of terms**

158 The interpretations of the terms (Fig. 1) employed in the descriptions of fossil scales

159 follow Andreev et al. (2015). The rationale behind this is to improve identification of

160 homologous scale structures across taxa by introducing a standardized terminology.

161

162 Results

163 **Systematic Palaeontology**

164   Class **CHONDRICHTHYES** Huxley, 1880

165   Order **MONGOLEPIDIDA** Karatajūtė-Talimaa, Novitskaya, Rozman & Sodov, 1990

166   **Included Families**

167   Mongolepididae Karatajūtė-Talimaa et al., 1990

168   Shiqianolepidae Sansom, Aldridge & Smith, 2000

169   **Emended diagnosis**

170   Polyodontode growing scale crowns formed by multiple antero-posteriorly oriented

171   primary odontocomplex rows. Odontode size within each row increases gradually

172   towards the posterior of the scale. Individual odontodes formed exclusively of

173   inotropically and spheritically mineralised atubular, acellular dentine (lamellin).

174   **Remarks**

175   The current study has determined scale crown growth (*sensu* Reif, 1978) to be a

176   characteristic shared by all mongolepid taxa (see Discussion for details), contrary to

177   previous interpretations of synchronomorial development of scale odontodes in

178   Mongolian mongolepid species (Karatajūtė-Talimaa et al., 1990; Karatajūtė-Talimaa &

179   Novitskaya, 1992, 1997). Under the revised definition of the Order, the Mongolepidida

180   retains the Families Mongolepididae (Karatajūtė-Talimaa et al., 1990) and

181   Shiqianolepidae (Sansom, Aldridge & Smith, 2000), yet *contra* Sansom, Aldridge &

182   Smith (2000) these are newly differentiated on the basis of base histology (see below)

183   and are expanded to also include the genera *Rongolepis* Sansom, Aldridge & Smith,

184   2000 and *Xinjiangichthys* Wang et al., 1998, respectively. *Solinalepis levis* gen. et sp.

185 nov. is also added to the Order, but placed within incertae sedis at Family-grade due

186 to the absence of clearly defined characters at this taxonomic level.

187

188 Family **MONGOLEPIDIDAE** Karatajūtė-Talimaa, Novitskaya, Rozman & Sodov, 1990

189 **Included genera**

190 *Mongolepis* Karatajūtė-Talimaa, Novitskaya, Rozman & Sodov, 1990

191 *Teslepis* Karatajūtė-Talimaa & Novitskaya, 1992

192 *Sodolepis* Talimaa & Novitskaya, 1997

193 *Rongolepis* Sansom, Aldridge & Smith, 2000

194 **Emended diagnosis**

195 Mongolepids possessing bulging scale bases composed of acellular bone tissue with

196 cross-ply architecture.

197 **Remarks**

198 Scale-derived phylogenetic data (Fig. 2; Andreev, Coates & Sansom, unpublished)

199 identify two monophyletic groups inside Mongolepidida distinguished by differences in

200 the bone histology and morphology of the scale base. These substitute the scale-

201 crown developmental characteristics that have been used previously by Sansom,

202 Aldridge & Smith (2000) to establish the Family structure of the Mongolepidida.

203

204 Genus *MONGOLEPIS* Karatajūtė-Talimaa, Novitskaya, Rozman & Sodov, 1990

205 **Type and only species**

206 *Mongolepis rozmanae* Karatajūtė-Talimaa *et al.* 1990, from the Chargat Formation,

207 Salhit regional Stage (Upper Llandovery–Lower Wenlock) of north-western Mongolia.

208 Non-figured *M. rozmanae* and *M.* sp. specimens have been reported (Sennikov et al.,

209 2015) from the Aeronian (Middle Llandovery) Sadra section (Gornaya Shoriya, Altai

210 Republic, Russia) and the Sheinwoodian (Lower Wenlock) Upper Tarkhata

211 Subformation (Charygka horizon, Gorny Altai, Altai Republic, Russia) and Baytal

212 Formation (Pichishui Horizon, Tuva Republic, Russia).

213 **Diagnosis**

214 As for the type species.

215

216 *MONGOLEPIS ROZMANAE* Karatajūtė-Talimaa, Novitskaya, Rozman & Sodov, 1990

217 (Figs. 1, 3A–D, 6A–E, 8A–C, 9D)

218 1990 *Mongolepis rozmanae* Karatajūtė-Talimaa, Novitskaya, Rozman & Sodov, figs.

219 2–5, pl. IX.

220 1992 *Mongolepis rozmanae* Karatajūtė-Talimaa & Novitskaya, fig. 2ж, з.

221 1995 *Mongolepis rozmanae* Karatajūtė-Talimaa, fig. 1.

222 1998 *Mongolepis rozmanae* Karatajūtė-Talimaa, figs. 11, 20.

223

Emended diagnosis

225 Mongolepidids (pertaining to Mongolepididae) possessing large scales (up to over 3

226 mm), constricted along their anterior margin, containing a large number of primary

227 odontocomplex rows (up to 50+) with long, sigmoidal odontodes. Inter-odontocomplex

228 spaces divided into pore-like compartments by short, transverse struts. Bulbous base

229 with a prominent crescent-shaped anterior platform that forms below the level of the

230 crown surface and extends laterally into two spine-shaped processes.

231 **Holotype**

232 An ontogenetically mature scale (LGI M-1-031) deposited in collection LGI M-1 of the

233 Lithuanian Geological Survey, Vilnius (Karatajūtė-Talimaa et al., 1990).

234 **Referred material**

235 Hundreds of isolated scales from the type locality (from samples P-16/3 and ЦГЭ

236 N1009). Non-figured specimens examined for this study are stored in the

237 microvertebrate research collection of the Lapworth Museum of Geology, University of

238 Birmingham, UK.

239 **Description**

240 **Morphology**

241 Primary odontodes from the same position in the crown are of equal size irrespective

242 of scale dimensions. The number of odontocomplex rows changes with the

243 proportions of the crown and its size, with scales of up to 2 mm in length usually

244 possessing less than 20 odontocomplexes, whereas in larger specimens their number

245 varies from 20 to c. 35.

246   Primary odontodes exhibit posteriorly curved profiles and an incremental

247 increase in length towards the posterior of the scale (Figs. 6A, B, 9D). This creates a

248 significant height difference (over five fold in medial odontocomplexes) between the

249 anterior- and the posterior-most elements of primary odontocomplexes, whilst

250 odontode thickness remains relatively constant at c. 50 μm (Figs. 6A, B, 9D). The

251 crown surface profile is planar (Fig. 3A, B, D) due to a gradual decrease in the angle

252 of odontode curvature towards the posterior of the scale, accompanied by sloping of

253 the crown/base contact surface (Figs. 6A, 9D).

254   In scales larger than 1 mm, secondary odontodes are developed to a varying

255 extent along the anterior margin of the crown (Fig. 3A, B, D). These are arranged into

256 rows and are undivided by inter-odontode spaces (Fig. 3A, B, D). In common with the

257 main crown odontodes, the secondary odontodes are posteriorly arched elements that

258 demonstrate an unidirectional increase in length (Figs. 6A–B, 9D); the latter being

259 expressed towards the anterior end of the scale.

260   The scale bases are bulbous structures (Fig. 3A–C) that reach their maximum

261 thickness directly under the anterior apex of the crown. To the posterior, the majority

262 of scale bases display a pitted lower-base surface produced by series of canal

263 openings (Fig. 3B, C).

264 **Histology**

265 Scale odontodes are composed of atubular dentine (Fig. 6A–C) for which Karatajūtė-

266 Talimaa et al. (1990) used the term lamellin (first introduced by Bolshakova and

267 Ulitina, 1985). Within individual odontodes, the lamellin displays two histologically

268 distinct regions—a peripheral (10–20 µm thick) lamellar zone and an inner region

269 dominated by mineralised spherites united within *Liesegang* waves (Fig. 6C; for a

270 definition refer to (Ørvig 1951)). The diameter of the calcospherites changes randomly

271 but rarely exceeds 15 µm.

272   Primary odontode pulps are either closed off or can be greatly constricted by

273 dentine infill (Figs. 6A, 8C) yet remaining open at their lower end, from which emerges

274 a pair of short (*c.* 15 µm) horizontal canals that connect the pulp cavity to the

275 odontode surface (Fig. 8C, C1). The foramina of these canals face either the inter-

276 odontocomplex spaces or, in marginal odontodes, are exposed at the periphery of the

277 crown (Fig. 3A).

278   In a similar manner to primary odontocomplexes, the pulps of secondary

279 odontodes are substantially constricted by dentine deposition, but they lack the

280 network of horizontal canals (Figs. 3A, B, 8C) developed inside the rest of the crown.

281   The scale base consists of acellular bone characterized by a succession of

282 convex-down growth lamellae (up to 150 µm thick; Fig. 6A, D, 9D) that increase in

283 extent towards the lower portion of the tissue. Secondary lamination is evident within

284 these primary depositional structures and is produced by intrinsic mineralised fibres

285 (*sensu* Ørvig, 1966) of *c.* 2 µm diameter, which likewise demarcate the boundary

286 surfaces of primary lamellae (Fig. 6D). The basal bone also contains elaborately

287   organised extrinsic crystalline fibres (*sensu* Ørvig, 1966) of *c*. 2 µm diameter (Fig. 6A,

288   E), which have the appearance of hollow cylindrical rods (Fig. 5E). These are grouped

289   into layers oriented obliquely with respect to one another (Fig. 6A, E, 9D), that

290   propagate through the tissue. The layers exhibit straight to upwardly arching profiles

291   and thickness of *c*. 50-70 µm (Fig. 6A, D, E; 9D).

292   The base houses a vascular system represented by curved (both anteriorly and

293   posteriorly) large-calibre vertical canals (*c*. 100 µm; Fig. 8A, B) that are split at their

294   upper end into two or more rami, each merging with one of the primary odontode

295   pulps. Conversely, the secondary odontode pulps are not connected to the canal

296   system of the base.

297   **Remarks**

298   In contrast to earlier work on *Mongolepis* (Karatajūtė-Talimaa et al., 1990; Karatajūtė-

299   Talimaa, 1998), the present study reinterprets the pattern of scale ontogenesis of the

300   genus. Recorded size differences between *Mongolepis* scales have been used by

301   previous authors (Karatajūtė-Talimaa et al., 1990; Karatajūtė-Talimaa, 1998) to

302   identify four distinct ontogenetic stages in the development of the scale cover. They

303   have suggested synchronomorial crown growth succeeded by incremental deposition

304   of basal bone to characterise the scale morphogenesis of *Mongolepis*, with scales of

305   ever-increasing crown size and base thickness assumed to be added at each stage of

306   scale cover ontogeny. A re-examination of *Mongolepis* specimens has revealed the

307   presence of bases across the spectrum of documented scale sizes. Furthermore,

308   specimens in the sub-millimetre size category, corresponding to the papillary and

309 juvenile scales of Karatajūtė-Talimaa et al. (1990), possess bases that are

310 proportionally as thick as those of larger scales. Thus, scales interpreted as being

311 composed exclusively of odontodes (Karatajūtė-Talimaa, 1998, fig. 11A2, E) were

312 related to specimens where the bases had been abraded away. This new

313 morphological evidence supports incremental and mutually synchronous deposition of

314 *Mongolepis* crown and base scale components. The odontocomplex structure and

315 base depositional lamellae of *Mongolepis* scales are similarly identified in all

316 mongolepid genera and indicate that cyclomorial scale growth, achieved via

317 sequential areal addition of odontodes (*sensu* Sansom, Aldridge & Smith (2000),

318 originally defined by Stensiö (1961)), is a characteristic of the Mongolepidida (see

319 Discussion for details).

320

321 Genus **TESLEPIS** Karatajūtė-Talimaa & Novitskaya, 1992

322 **Type and only species**

323 *Teslepis jucunda* Karatajūtė-Talimaa & Novitskaya, 1992, from the Chargat Formation

324 (Salhit regional Stage, Upper Llandovery–Lower Wenlock) of north-western Mongolia.

325 Non-figured *T. jucunda* specimens have been reported (Sennikov et al., 2015) from

326 the Aeronian (Middle Llandovery) Sadra section (Gornaya Shoriya, Altai Republic,

327 Russia) and the Sheinwoodian (Lower Wenlock) Upper Tarkhata Subformation

328 (Charygka horizon, Gorny Altai, Altai Republic, Russia).

329 **Diagnosis**

330   As for the type species.

331

332   *TESLEPIS JUCUNDA* Karatajūtė-Talimaa & Novitskaya, 1992

333   (Figs. 3E–G, 6F, 8D, 9A)

334   1992 *Teslepis jucunda* Karatajūtė-Talimaa & Novitskaya, figs. 1, 2a–e, 3, 4, pl. V figs.

335   1–8.

336   1992 *Teslepis* sp. Karatajūtė-Talimaa & Novitskaya, pl. V fig. 9.

337   1998 *Teslepis jucunda* Karatajūtė-Talimaa, fig. 19.

338   **Emended diagnosis**

339   Mongolepidids with small scales whose odontocomplex number increases with scale

340   size. Non-odontode atubular globular dentine developed at the anterior and lateral

341   crown margins. Scale base extended into an antero-basally directed conical

342   projection.

343   **Holotype**

344   An ontogenetically mature scale (LGI M-1-077) deposited in collection LGI M-1 of the

345   Lithuanian Geological Survey, Vilnius (Karatajūtė-Talimaa & Novitskaya, 1992).

346   **Material**

347   Several hundred isolated scales from the type locality (from samples P-16/3 and ЦГЭ

348   N1009). Non-figured specimens examined for this study are stored in the

349   microvertebrate research collection of the Lapworth Museum of Geology, University of

350   Birmingham, UK.

351

Description

Morphology

354 The number of the scale odontocomplex rows is related to crown size and its

355 proportions. In small specimens (less than 0.5 mm long) their number varies from 4 to

356 6, whilst it reaches 17 in scales larger than 1 mm. Within the individual

357 odontocomplexes the odontode length gradually increases in a posterior direction (Fig.

358 6F), whereas odontode thickness remains relatively constant at *c*. 50 μm.

359 In the majority of specimens a crescent-shaped platform (Fig. 3E, F) is formed

360 anterior to the odontocomplexes, and the former can be elevated slightly above the

361 level of the odontodes. The absence of this thickening does not correlate with a

362 particular scale size.

363 The base is not constricted at the contact with the crown (Fig. 3E–G) and

364 extends away from this junction into an anteriorly-directed conical projection that

365 protrudes beyond the crown margin. The posterior third of the base is shallower in

366 comparison with its thickened anterior (Fig. 6F), and is marked by rows of canal

367 openings (30–60 μm in diameter; Fig. 3G) aligned with the odontocomplexes of the

368 crown.

Histology

370 The crown odontodes consist of atubular dentine (lamellin; Fig. 6F) having a

371 predominately lamellar periphery and an inner spheritically mineralised region. The

372 calcospherites of the globular lamellin attain a diameter of approximately 10 μm and

373 comprise of concentric *Liesegang* rings closed around a central cavity. These exhibit

374 linear or concave arrested growth contact surfaces with other spherites and adjacent

375 *Liesegang* waves. The scale odontodes possess vascular spaces in the form of

376 vestiges of pulp canals that are mostly filled by lamellin. The pulps branch out laterally

377 as paired short horizontal canals (diameter 10–15 μm) that open on the odontode

378 surface (Fig. 8D, D1).

379   A structural variety of atubular dentine different from lamellin forms the crown

380 platform that surmounts the thickest part of the base (Fig. 6F). This tissue exhibits

381 exclusively spheritic mineralisation represented by tightly packed globules (up to 10

382 μm in diameter), and lacks a canal system.

383   The basal bone is acellular with a series of depositional lamellae demarcated

384 by basally arched intrinsic fibres (Fig. 6F). The smallest lamellae reside at the level of

385 the anterior-most odontodes, with lamella thickness varying from 15 μm to 20 μm

386 across the extent of the tissue.

387   The basal bone contains extrinsic mineralised fibres grouped into 20–40 μm

388 thick layers with upwardly curved profiles. The fibres within each layer are mutually

389 parallel but also oriented obliquely to those of adjacent lamellae, giving the bone a

390 plywood-like texture. In addition to the abundant fibres with layered organization, the

391 tissue contains a set of extrinsic, vertically oriented fibres (Fig. 6F) that are evenly

392 spaced at about 5 μm intervals and propagate up to the level of the crown-base

393 junction.

394   The base is penetrated by a number of large-calibre vertical vascular canals

395   (Fig. 8D, D1), which connect with the pulp cavities of crown odontodes. The former

396   are predominantly preserved in the posterior (thinnest) third of the base as anteriorly

397   arching canals that gradually widen to c. 40 μm at the lower base surface (Fig. 8D,

398   D1).

399   **Remarks**

400   The anterior crown platform of *Teslepis* scales (developed also in *Sodolepis*) received

401   little attention in the descriptions of Karatajūtė-Talimaa & Novitskaya (1992) and

402   Karatajūtė-Talimaa (1998), apart from being identified as composed of an

403   undetermined type of globular basal tissue. The platform always forms at the level of

404   the primary odontodes and sutures to the anterior most of them, developing in the

405   space typically occupied by secondary odontodes in *Mongolepis*, *Rongolepis*,

406   *Xinjiangichthys* and *Shiqianolepis* scales. From a histological perspective, the lack of

407   lamellar matrix and the predominantly arrested-growth contact surfaces of spherites

408   resemble the microstructure of certain types of spheritically mineralized dentine

409   (Schmidt & Keil, 1971, fig. 46, 47). Consequently, this tissue is regarded to be globular

410   atubular dentine as opposed to globular dermal bone that is commonly formed only in

411   the cavity-rich cancellous zone of the exoskeleton of lower vertebrates (Ørvig, 1968;

412   Donoghue, Sansom & Downs, 2006; Downs & Donoghue, 2009).

413   Contrasting with the well-defined and consistent shape of the odontodes, the

414   anterior platform has an irregular surface and poorly defined boundaries, and whose

415   shape is determined by the contours of the underlying base. As a consequence, it

416 could be suggested that this mass of globular dentine is not the product of a well-

417 differentiated dermal papilla, which typifies early odontode development and

418 determines the morphology of odontodes independently of that of the basal bone

419 (Sire, 1994; Sire & Huysseune, 1996; Sire & Huysseune, 2003). Outside *Teslepis* and

420 *Sodolepis*, dentine structures with similar characteristics have not been documented in

421 the integumentary skeleton of gnathostomes.

422   Cellular basal bone was considered by Karatajūtė-Talimaa & Novitskaya (1992)

423 to be a diagnostic characteristic of *Teslepis* in the original description of the genus.

424 Fusiform odontocyte lacunae identified in that study are considered herein to

425 represent hollow interiors of mineralised fibres of within bone matrix (the implications

426 of this revised interpretation are expanded on in the Discussion).

427

428 Genus **SODOLEPIS** Karatajūtė-Talimaa & Novitskaya, 1997

429 **Type and only species**

430 *Sodolepis lucens* Karatajūtė-Talimaa & Novitskaya, 1997, from the Chargat Formation

431 (Salhit regional Stage, Upper Llandovery–Lower Wenlock) of north-western Mongolia.

432 **Diagnosis**

433 As for the type species.

434

435 **SODOLEPIS LUCENS** Karatajūtė-Talimaa & Novitskaya, 1997

436   (Figs. 3H–J, 6G–J, 8E)

437   1997 *Sodolepis lucens* Karatajūtė-Talimaa & Novitskaya, figs. 1–3, pl. XI.

438   1998 *Sodolepis lucens* Karatajūtė-Talimaa, fig. 18.

439   **Emended diagnosis**

440   Mongolepidids with medium-sized scales (up to over 2 mm) possessing crowns

441   composed of sutured odontocomplex rows, whose number does not increase with

442   scale size. Anterior crown platform of globular dentine elevated to the level of the

443   crown surface. Neck (horizontal) canals not formed at the lower portion of crown

444   odontodes.

445   **Holotype**

446   An isolated scale with accession number LGI M-1-091 deposited in collection LGI M-1

447   of the Lithuanian Geological Survey, Vilnius (Karatajūtė-Talimaa & Novitskaya, 1997).

448   **Referred material**

449   More than a hundred isolated scales from the type locality (samples P-16/3 and ЦГЭ

450   N1009). Non-figured specimens examined for this study are stored in the Lapworth

451   Museum of Geology, University of Birmingham, UK.

452   **Remarks**

453   The gross morphology of *Sodolepis* scales (Fig. 3H–J) closely resembles that of

454   *Teslepis*, with the two genera demonstrating comparable histology. The latter,

455   however, are distinguished on the basis of differences in odontode size and crown

456 vascularization. *Sodolepis* crowns possess fused odontocomplexes, composed of

457 odontodes that are on average three times as large of those of *Teslepis*, divided by

458 inter-odontocomplex spaces. This is due to a corresponding increase of odontode and

459 scale size in *Sodolepis*, leading to the formation of a relatively constant number of

460 odontocomplexes irrespective of crown dimensions. In *Teslepis* specimens, on the

461 other hand, odontode size remains consistent across all documented scale lengths.

462   As noted by Karatajūtė-Talimaa & Novitskaya (1997), a system of horizontal

463 canals cannot be identified inside *Sodolepis* scale crowns (Fig. 8E)—an atypical

464 condition considering that the majority of mongolepid genera, including *Teslepis*,

465 develop some type of pulp canal openings on the lower crown surface.

466

467 Genus ***RONGOLEPIS*** Sansom, Aldridge & Smith, 2000

468 **Type and only species**

469 *Rongolepis cosmetica* from the Telychian (Upper Llandovery) of south China, Lower

470 Member of the Xiushan Formation (Sansom, Aldridge & Smith, 2000) and the

471 Telychian of Bachu County, Xinjiang, China (Lower member of the Yimugantawu

472 Formation; N-Z Wang, unpublished data).

473 **Diagnosis**

474 As for the type species.

475

476   ***RONGOLEPIS COSMETICA*** Sansom, Aldridge & Smith, 2000

477   (Figs. 3K–M, 6K, L)

478   2000 *Rongolepis cosmetica* Sansom, Aldridge & Smith, figs. 11, 12.

479   **Emended diagnosis**

480   Mongolepidid species with scale odontocomplex rows ornamented by narrow median

481   ridges, flanked anteriorly and laterally by conical secondary odontodes. Posterior

482   primary odontodes long and straight, having pitted by rows of foramina on their lower

483   crown face. Base tetragonal or oblong, displaced towards the scale anterior. Lower

484   base surface concave to flat with a central conical projection.

485   **Holotype**

486   An isolated scale (NIGP 130326) from the Xiushan Formation of south China

487   (Sansom, Aldridge & Smith, 2000).

488   **Referred material**

489   Hundreds of specimens from the Xiushan Formation of Leijiatun (Shiqian county,

490   south China (sample Shiqian 14B), including type series material (NIGP 130319–

491   NIGP 130330) figured by Sansom, Aldridge & Smith (2000). Non-figured specimens

492   stored in the Nanjing Institute of Geology and Palaeontology, Chinese Academy of

493   Sciences, Nanjing, China.

494   **Remarks**

495   The uncertainty regarding the supergeneric position of *Rongolepis* in the original

496   description of the genus (Sansom, Aldridge & Smith, 2000) has been attributed to a

497   suite of characteristics (scale morphology, posterior of the crown composed of

498   acellular lamellar bone and presence of crown odontodes) not known in the scales of

499   other vertebrates. The re-examination of *Rongolepis cosmetica* has enabled the

500   identification of a combination of features diagnostic for Mongolepidida. Of particular

501   importance in this regard is the nature of the tissue composing the flared posterior

502   extension of *Rongolepis* scales. Suggested to be formed of lamellar bone (Sansom *et*

503   *al.* 2000), this portion of the scale in fact demonstrates the lamellin-type architecture of

504   an inotropically and spheritically mineralized (for definitions of both see Ørvig, 1968

505   and Zylberberg et al. 1992) atubular tissue devoid of attachment fibres (Fig. 6K, L).

506   Moreover, the segmentation of the crown's posterior part observed in thin sections

507   (Fig. 6K, L; Sansom, Aldridge & Smith, 2000, fig. 12e) is interpreted to be produced by

508   the contact surfaces of sutured odontodes. Both the anterior to posterior increase in

509   length of these elements and their arrangement in longitudinal rows over the posterior

510   half of the base are known features of mongolepid primary odontocomplexes. The

511   assignment of *Rongolepis* to Mongolepidida is thus dictated by the possession of its

512   scales of lamellin and polyodontocomplex growing crowns.

513

514   Family **SHIQIANOLEPIDAE** Sansom, Aldridge & Smith 2000

515   **Included Genera**

516   *Xinjiangichthys* Wang et al., 1998 and *Shiqianolepis* Sansom, Aldridge & Smith, 2000.

517   **Emended diagnosis**

518   Mongolepids with scale bases composed of non-vascular, cellular bone tissue.

519

520   Genus *SHIQIANOLEPIS* Sansom, Aldridge & Smith, 2000

521   **Type and only species**

522   *Shiqianolepis hollandi* Sansom, Aldridge & Smith, 2000, from the Telychian Lower

523   Member of the Xiushan Formation (Leijiatun, Shiqian county, southern China).

524   **Emended diagnosis**

525   As for the type species.

526

527   *SHIQIANOLEPIS HOLLANDI* Sansom, Aldridge & Smith, 2000

528   (Figs. 4A–C, 5N, 8F, 9B, E)

529   2000 *Shiqianolepis hollandi* Sansom, Aldridge & Smith, figs. 4–6.

530   **Emended diagnosis**

531   Shiqianolepids with trunk scale odontocomplexes separated posteriorly by deep inter-

532   odontocomplex spaces. A cluster of tightly sutured secondary odontodes formed

533   anteriorly of crown odontocomplexes. Crown surface ornamented by tuberculate

534   ridges. Oblong asymmetrical head scales (up to 1 mm long) with irregularly-shaped

535   odontodes distributed peripherally around a medial ridge.

Holotype

537   An isolated trunk scale (NIGP 130294) from the Xiushan Formation of Leijiatun (Shiqian

538   County) south China (Sansom, Aldridge & Smith, 2000).

Referred material

540   Hundreds of isolated scales and type series specimens (NIGP 130293–NIGP 130318)

541   figured by Sansom, Aldridge & Smith (2000) from the Telychian Xiushan Formation

542   (sample Shiqian 14B) of Leijiatun (Shiqian county, south China). Non-figured material

543   stored in the Nanjing Institute of Geology and Palaeontology, Chinese Academy of

544   Sciences, Nanjing, China.

Remarks

546   Characteristic for *Shiqianolepis* scales is a distinct primordial odontode located at the

547   apex of the conical base. This odontode has been termed 'proto-scale' by Sansom,

548   Aldridge & Smith (2000) and was identified as a diminutive element overlain by the

549   much larger odontodes deposited at later stages of crown ontogeny. Superpositional

550   growth, which results in odontodes not being exposed on the crown surface, is a

551   condition atypical for other mongolepids, also demonstrated to not be a feature of

552   *Shiqianolepis* scales. Upon re-examination of figured material and newly sectioned

553   specimens, the primordial odontode borders recognized in Sansom, Aldridge & Smith

554   (2000, figs. 6b, 7) are now considered to constitute the margins of dentine depositional

555   lamellae (Fig. 6N), as these are occasionally observed to be indented by more

556   peripherally formed calcospherites—evidencing a centripetal mode of dentine

557   histogenesis as opposed to stacking of primary odontodes. As identified here, the

558   primordial odontode in *Shiqianolepis* scales is overlapped only at its anterior end by

559   secondary odontodes, whilst most of its upper margin remains exposed on the crown

560   surface. Similarly to the rest of the odontocomplexes of *Shiqianolepis* trunk scales, the

561   one incepted by the 'proto-scale' also displays a gradual posterior increase of

562   odontode size.

563

564   Genus **XINJIANGICHTHYS** Wang, Zhang, Wang & Zhu, 1998

565   **Type and only species**

566   *Xinjiangichthys pluridentatus* Wang, Zhang, Wang & Zhu, 1998, from the Telychian

567   Yimugantawu Formation (north-western margin of the Tarim Basin, Xinjiang, PR

568   China).

569   **Emended diagnosis**

570   As for the type species.

571   **Remarks**

572   The placement of *Xinjiangichthys* inside Mongolepidida by Wang et al. (1998) was

573   justified on the grounds of similarities in crown morphology and odontode patterning

574   with Mongolian mongolepids (the only known mongolepid taxa at the time of its

575   description), and this study advances that claim further by identifying a

576   polyodontocomplex crown structure in *Xinjiangichthys* scales.

577   The presence of atubular dentine in *Xinjiangichthys* scales, another of the

578   diagnostic characters of mongolepids (this study; Karatajūtė-Talimaa et al., 1990;

579   Sansom, Aldridge & Smith, 2000), can be determined in thin-section (Fig. 6M) and

580   through X-ray microtomography (Fig 8G, H).

581   Furthermore, Wang et al.'s (1998) interpretation of *Xinjiangichthys* scale bases

582   as non-growing is rejected here by the recognition of a conical basal tissue that

583   supports, at its apex, the primordial odontode and further posteriorly the rest of the

584   scale's primary odontodes, similarly to the growing bases of *Shiqianolepis* and those

585   of mongolepids in large (Fig. 6M; Fig. 8H).

586

587   ***XINJIANGICHTHYS PLURIDENTATUS*** Wang, Zhang, Wang & Zhu, 1998

588   (Figs. 4D–F, 6M, 8G–H)

589   1998 *Xinjiangichthys pluridentatus* Wang, Zhang, Wang and Zhu, pl. 1, fig. a–d.

590   1998 *Xinjiangichthys tarimensis* Wang, Zhang, Wang & Zhu, pl. 1, fig. e–i.

591   v. 2000 *Xinjiangichthys* sp. Sansom, Aldridge and Smith, 236, fig. 8.

592   **Emended diagnosis**

593 Shiqianolepids with unornamented scale crowns composed of sutured odontocomplex

594 rows. Needle-like primary odontodes; erect, conical secondary odontodes.

Holotype

596 An isolated trunk scale (IVPP V11663.1) from the Yimugantawu Formation of Xinjiang

597 (Bachu county), China (Wang et al., 1998).

Referred material

599 Two specimens from the Telychian Xiushan Formation (Leijiatun, Shiqian county,

600 south China; sample Shiqian 14B), in addition to material figured (NIGP 130291, NIGP

601 130292) in Sansom, Aldridge & Smith (2000), and five specimens (including IVPP V

602 X1, IVPP V X2) from the Yimugantawu Formation (Bachu county, Xinjiang, PR China).

603 Non-figured scales are stored in the Nanjing Institute of Geology and Palaeontology,

604 Chinese Academy of Sciences, Nanjing, China and the Institute of Vertebrate

605 Paleontology and Paleoanthropology, Chinese Academy of Sciences, Beijing, China.

Remarks

607 *X. tarimensis* and *X.* sp. are synonymised with *X. pluridentatus* based on the absence

608 of differentiating characteristics between the specimens attributed to the two species.

609 The arguments (equal-sized crown odontodes, scale neck and pitted sub-crown

610 surface) of Wang et al. (1998) for erecting *X. tarimensis* are considered not valid for

611 the following reasons. The large-diameter anterior odontodes of *X. pluridentatus*

612 specimens figured by Wang et al. (1998, pl. Ia, c) represent secondary odontodes not

613 developed in all scales of the species (specimens identified as *X. tarimensis* by Wang

614   et al., 1998, pl. Ie-i), which is consistent with the condition documented in *Mongolepis*

615   (this study and Karatajūtė-Talimaa et al., 1990). The presence of secondary

616   odontodes also accounts for the lack of a distinct neck in the *Xinjiangichthys* scales

617   they develop, by occupying the sloped anterior surface of the base. The third

618   character considered diagnostic for *X. tarimensis* by Wang et al. (1998) are the

619   numerous foramina present on the lower crown surface of scales, which are also seen

620   (Figs. 4D, E, 8G–H) in *Xinjiangichthys* specimens with secondary odontodes.

621

622   Family incertae sedis

623   Genus **SOLINALEPIS** gen. nov.

624   **Type and only species**

625   *Solinalepis levis* gen. et sp. nov.

626   **Derivation of name**

627   From 'solinas' (tube, pipe in Greek), pertaining to the shape of the scale odontodes of

628   the species, and 'lepis', scale in Greek.

629   **Diagnosis**

630   As for the type species.

631   **Remarks**

632 Characters relating to the dimensions of the scale base (its extent and thickness in

633 relation to those of the crown) unite *Solinalepis* gen. nov. (data from yet to be

634 published phylogenetic analysis by Andreev, Coates & Sansom, unpublished; Fig. 2)

635 in a clade with members of Shiqianolepidae. Nevertheless, this type of morphological

636 data is not regarded informative at a supra-generic level and the genus is classified

637 outside the two recognized mongolepid families due to differences in scale base

638 histology (acellular bone lacking plywood-like organization of its mineralised matrix).

639 As a consequence, *Solinalepis* gen. nov. is treated as Mongolepidida *incertae sedis*.

640

641 ***SOLINALEPIS LEVIS*** sp. nov

642 (Figs. 5, 7, 8I–J, 9C)

643 2001 '?Mongolepid scales' Sansom, Smith and Smith, p. 161, fig. 10.3g, h.

644 2002 Unnamed chondrichthyan Donoghue and Sansom, p. 362, fig. 6.3.

645 2009 Stem-chondrichthyan Sire, Donoghue and Vickaryous, p. 424, fig. 10c.

646 **Derivation of name**

647 From the Latin 'levis' (smooth), referring to the unornamented scale crown surface of

648 the species.

649 **Locality and horizon**

650 The type locality is the vicinity of the Harding Quarry, situated c. 1 km west of Cañon

651 City (Fremont County, Colorado, USA). All *Solinalepis* specimens come from

652 Sandbian strata (Mohawkian regional series, *Phragmodus undatus* conodont zone) of

653 the Harding Sandstone (samples H94-26 and H96-20).

654 **Holotype**

655 An isolated trunk scale BU5310 (Fig. 5E).

656 **Referred material**

657 Hundreds of isolated scales, including BU5307–BU5318, BU5345.

658 Non-figured specimens examined for this study are stored in the microvertebrate

659 research collection of the Lapworth Museum of Geology, University of Birmingham,

660 UK.

661 **Diagnosis**

662 Mongolepid species with trunk scales crowns composed of tubular odontodes

663 organized in sutured longitudinal odontocomplex rows. Acellular basal bone housing

664 an elaborate canal system that opens via foramina on the basal surface. Radially

665 arranged tuberculate to conical head-scale odontodes.

666 # Description

667 **Morphology of head scales**

668 Polyodontode symmetrical or asymmetrical scales with height between 0.5 and 1.3

669 mm. These are represented by two main morphological variants, a compact, bulbous

670   type (Fig. 5D) and tessera-like scales (Fig. 5A–C) of larger diameter. Both

671   morphotypes possess irregular crowns composed of radially ordered odontodes, and

672   do not clearly exhibit distinct anterior, posterior and lateral scale faces. The radiating

673   odontodes form rows (five to nine odontodes long), offset in a manner in which the

674   odontodes of each row oppose the inter-odontode contacts of neighbouring

675   odontocomplexes. Odontode height diminishes gradually towards the crown centre,

676   accompanied by an increase of coalescence between odontodes.

677   The scales exhibit a prominent central bulge, away from which the crown

678   surface slopes down to the scale margin. In crown view, the latter has a corrugated

679   outline that in certain specimens is accentuated by deep, peripherally expanding

680   grooves (Fig. 5A, B).

681   The scale base displays a granular, grooved surface and follows the outline of

682   the crown. At its centre the base attains maximal thickness (Fig. 7A), and gradually

683   decreases in height away from this point. The lower-base surface is predominantly

684   planar or can have a moderate central concavity, but never exhibits the convex

685   topology documented in trunk scale specimens.

686   **Morphology of trunk scales**

687   The length of these scales varies between 100–400 μm and is always less (up to

688   three quarters) than their width. Specimens with crown lengths near or exceeding 200

689   μm demonstrate polygonal (Fig. 5E–G), often asymmetrical (Fig. 5F, G), outlines. The

690   anterior crown margin of these scales is typically wedge-shaped whilst their posterior

691   face is straight (Fig. 5I). In contrast, the crowns of antero-posteriorly short (100–200

692   µm long) scales tend to be symmetrical, leaf-shaped structures (Fig. 5J–L), rarely

693   demonstrating simple geometrical profiles in crown view.

694   Irrespective of crown morphology, the odontodes of trunk scales are organized

695   into closely packed antero-posteriorly aligned rows (Figs 5F–G, J, 9C). Adjacent rows

696   are displaced by approximately half an odontode diameter (c. 15 µm), resulting in an

697   offset between the odontodes of neighbouring odontocomplexes (Fig. 9C). The

698   odontodes themselves are cylindrical, tube-like elements with sigmoidal profiles that

699   taper to a point apically (Fig. 5J). Odontode length increases gradually towards the

700   scale's posterior end, where the crown can reach a height of *c*. 400 µm.

701   The crown/base transition is not marked by a neck-like constriction (Fig. 5E–L),

702   with the base never attaining more than a third of the overall scale height. The basal

703   surface is typically marked by deeply incised grooves (Fig. 5E–I) that give it a dimpled

704   appearance, characteristic also for the lower base surface. The latter has a

705   predominantly flat profile but can exhibit a central conical projection that is particularly

706   well developed in leaf-shaped specimens (Fig. 5L).

707   **Histology of head scales**

708   Due to diagenetic alteration of histologically examined scales, the microstructure of

709   crown odontodes is largely obscured. Nevertheless, wide odontode pulp canals are

710   evident in sectioned specimens (Fig. 7A), and these appear to end blindly inside the

711   crown. The upper base surface is perforated by a row of foramina (Fig. 5C, D) similar

712   to the ones documented in trunk scales.

713   The main structural components of the basal bone matrix are tightly packed, parallel

714   crystalline mineralized fibres with horizontal orientation (Fig. 7A). These are crosscut

715   by apically converging fibre bundles (up to 15 µm in diameter), which follow undulating

716   paths across the tissue.

717   **Histology of trunk scales**

718   Crown odontodes are structured out of atubular dentine (lamellin; Fig. 7B) that is

719   spherically mineralised in proximity of the pulp (spherite diameter 10–15 µm).

720   Cylindrical, non-branching pulp cavities occupy the centre of odontodes and are

721   connected at their lower ends with the canal system of the base (Fig. 8I, J). The latter

722   is represented by vertical canals that bifurcate close to the crown-base junction, with

723   each pair of rami re-connecting deeper inside the base, resulting in the formation of a

724   series of vascular loops (Fig. 8I, J). Vertically oriented canals emerge from the looped

725   canal system and open on the lower base surface. The basal surface is similarly

726   marked by numerous foramina that are the exit points for the peripheral canals of the

727   base (Fig. 5H).

728   The base is composed of acellular bone demonstrating the presence of *c.* 2 µm thick

729   extrinsic crystalline mineralised fibres that propagate vertically through the tissue (Fig.

730   7B).

731   **Remarks**

732   The development of polyodontocomplex scale crowns formed from lamellin identify

733   *Solinalepis levis* gen. et sp. nov. scales as a mongolepid species. Moreover, the trunk

734   scale odontocomplexes of *Solinalepis* gen. nov. exhibit the same progressive posterior

735   increase in odontode length documented in members of the Order.

736   Within Mongolepidida, the combination of a large odontocomplex number (>20)

737   and sutured odontodes is present only in the Telychian genus *Xinjiangichthys*.

738   Nevertheless, the two taxa are readily distinguished on the basis of base histology and

739   canal-opening distribution on the scale surface. In addition to that, *Solinalepis* gen.

740   nov. is one of only two described mongolepid genera (the other being *Shiqianolepis*)

741   known to develop with squamation clearly differentiated into distinct trunk (exhibiting

742   recognizable anterior and posterior faces) and head morphotypes (irregular-shaped

743   elements)—a condition that is consistent with that recorded in a number of

744   heterosquamous Lower Palaeozoic gnathostomes known from articulated specimens

745   (e.g. *Climatius reticulatus* Miles, 1973, *Obtusacanthus corroconius* Hanke & Wilson,

746   2004, *Gladiobranchus probaton* Hanke & Davis, 2008 and *Ptomacanthus anglicus*

747   Miles, 1973; Brazeau, 2012).

748

DISCUSSION

749

Crown morphogenesis of mongolepid scales

750

751   *Shiqianolepis hollandi* is recognized as a key taxon for determining the mode of scale

752   crown development in mongolepids, following the identification by Sansom, Aldridge &

753   Smith (2000) of 'proto-scale' (early-development phase) specimens of the species

754   (Sansom, Aldridge & Smith, 2000, fig. 4u, w). The size (half of that of 'mature' trunk

755 scales) and the small number of crown odontodes (exhibiting only the earliest formed

756 odontodes of incipient primary odontocomplexes) of these scales implies that in

757 *Shiqianolepis* scale ontogenesis involves crown enlargement through sequential

758 addition of odontodes. Significantly, this style of crown architecture (primary

759 odontocomplex rows originating at the most elevated point of the base and

760 characterized by a posterior increase in size of their constituent odontodes) is

761 developed in all members of the Mongolepidida (Figs. 6A, F, I, K, M, N, 9) and is

762 evidence that the mongolepids share a cyclomorial pattern of scale ontogenesis.

763   Data from developmental studies on extant neoselachians indicate that their

764 scales cannot serve as model systems for determining the mechanism of

765 morphogenesis of the compound mongolepid scale crowns, as the former have been

766 shown to be simple monodontode elements produced by a single epithelio-

767 ectomesenchymal primordium (Schmidt & Keil, 1971; Reif, 1980, Miyake et al., 1999;

768 Sire & Huysseune, 2003; Johanson, Smith & Joss, 2007; Johanson et al., 2008).

769 Examinations of multiple odontode generation in osteichthyan scales (Kerr, 1952;

770 Smith, Hobdell & Miller, 1972; Smith, 1979; Sire & Huysseune, 1996), though, provide

771 insight into the timing of deposition of odontode aggregations associated with a dermal

772 bone support tissue. They reveal phases of odontode generation that result in an

773 increase of odontode number throughout scale ontogeny.

774   The proposed scale growth mechanism in Mongolepidida is further

775 substantiated by evidence from the Palaeozoic record of the Chondrichthyes. The

776 scale crown structure of certain euchondrichthyan taxa described from articulated

777 specimens (e.g. *Diplodoselache woodi* Dick, 1981, *Tamiobatis vetustus* Williams,

778   1998 and *Orodus greggi* Zangerl, 1968), conform closely to the odontode patterning of

779   mongolepid scales. *Diplodeselache* trunk scales were noted by Dick (1981) to closely

780   resemble those of *Orodus* and to be similarly characterized by cyclomorial growth.

781   Previous work (Reif, 1978) on the morphogenesis of the chondrichthyan

782   integumentary skeleton also recognized sequential crown elongation through regular

783   addition of odontodes as the mechanism of scale development in *Orodus*. This pattern

784   of crown formation is also typical for scales with a *Ctenacanthus costellatus* type of

785   morphogenesis (defined by Reif, 1978 and equivalent to the *Ctenacanthus* B3

786   morphogenetic type of Karatajūtė-Talimaa, 1992) to which *Tamiobatis* scales have

787   been attributed (Williams, 1998).

Mongolepid scale crown histology

789   The emergence of skeletal mineralisation in vertebrates (Donoghue & Sansom, 2002;

790   Donoghue, Sansom & Downs, 2006) coincides with the origin of atubular dentine-like

791   tissues that compose the basal bodies of certain conodont genera (Sansom, 1996;

792   Smith, Sansom & Smith, 1996; Donoghue, 1998; Dong, Donoghue & Repetski, 2005).

793   Conodont atubular 'dentines' frequently exhibit (Sansom 1996, fig. 2e–h; Donoghue,

794   1998, fig. 5a–c; Dong, Donoghue & Repetski, 2005, pl. 1, figs 3–9) peripheral lamellar

795   fabric, substituted internally by spheritically mineralised matrix, making them

796   structurally (but not phylogenetically) comparable with the architecture of mongolepid

797   lamellin (Fig. 6C, G). The conodont tissues have recently been hypothesized to have

798   arisen in a stepwise manner in the oropharyngeal skeleton of the Paraconodonta and

799   Euconodonta (Murdock et al., 2013), whilst separately, within the Total Group

800 Gnathostomata the known occurrence of atubular dentines outside the Mongolepidida

801 is limited to the scale odontodes of the pteraspidomorph *Tesakoviaspis concentrica*

802 (Karatajūtė-Talimaa & Smith, 2004) and the fin spine ornament of sinacanthid

803 gnathostomes (Sansom, Aldridge & Smith, 2000; Sansom, Wang & Smith, 2005).

804 An important aspect of the atubular nature of lamellin is that it provides circumstantial

805 evidence for the involvement of atypical (from a modern perspective) odontoblasts in

806 the generation of the tissue. During dentinogenesis mature odontoblasts commonly

807 extend long cellular processes into the mineralised phase, which remain contained

808 inside tubular spaces after formation of the tissue is complete (Linde, 1989; Linde &

809 Lundgren, 1995; Yoshiba et al., 2002; Magloire et al., 2004, 2009). The inability of

810 secretory odontoblasts to form dentinal tubules is taken to suggest that such cells

811 either did not embed their processes within the dentine matrix at any depth or lacked

812 processes altogether. Atypical odontoblasts devoid of large cytoplasmic projections

813 have been reported in the tooth germs of the Recent sting ray *Dasyatis akajei*

814 (Sasagawa, 1995), but these are found to co-exist with unipolar odontoblasts,

815 characterized by well-developed processes. The apical portions of odontoblasts and

816 their processes have been implicated as ion channel-rich sites capable of being

817 activated by environmental stimuli via tubular fluid movement, and are presumably

818 involved in transmitting sensory input to pulp nerve endings (Okumura et al., 2005;

819 Allard et al., 2006; Magloire et al., 2009). This raises the possibility that mongolepid

820 scale pulps had limited ability to transduce sensory input compared with an

821 odontoblast population that forms tubular network inside a mineralised dentine matrix.

822 **Histology of mongolepid scale bases**

823   This and previous studies (Karatajūtė-Talimaa et al., 1990; Karatajūtė-Talimaa 1995;

824   Karatajūtė-Talimaa & Novitskaya, 1992, 1997; Sansom, Aldridge & Smith, 2000)

825   identify mongolepid scale odontodes to be supported by a common base composed of

826   lamellar bone (Fig. 6A, F, H, I, K, M, N, 7). The basal tissue of *Mongolepis* and

827   *Sodolepis* scales has been interpreted as acellular bone (Karatajūtė-Talimaa et al.,

828   1990; Karatajūtė-Talimaa & Novitskaya, 1997), with this study also recognizing the

829   absence of osteocyte lacunae in the bases of *Teslepis* (*contra* Karatajūtė-Talimaa &

830   Novitskaya, 1992), *Rongolepis* (in agreement with Sansom, Aldridge & Smith, 2000)

831   and *Solinalepis* gen. nov.—restricting the occurrence of cellular bone inside

832   Mongolepidida to the genera *Xinjiangichthys* and *Shiqianolepis* (this study and

833   Sansom, Aldridge & Smith, 2000).

834   A cross-ply layering of crystalline fibres is recognized as the predominant type

835   of basal bone texture of mongolepid scales, being documented in the four genera of

836   the Family Mongolepididae. This architecture of the mineralised matrix matches

837   closely the organization of the collagen fibres in the deep dermis (stratum compactum)

838   of extant neoselachians (Motta 1977; Miyake et al., 1999; Sire & Huysseune, 2003)

839   and osteichthyans (Kerr, 1952, 1955; Sire, 1993; Gemballa & Bartsch, 2002) and is

840   suggested to be indicative of dermal bone histogenesis achieved through

841   mineralisation of the a largely unmodified fibrous scaffold of the stratum compactum—

842   a process referred to as metaplastic ossification (Sire, 1993; Sire, Donoghue &

843   Vickaryous, 2009). Consequently, the observed absence of cross-ply layering in the

844   cellular bone of mongolepid scale bases (in *Xinjiangichthys*, *Shiqianolepis* and

845   *Solinalepis* gen. nov.) could be interpreted to result from remodeling of the original

846   fibrous framework of stratum compactum prior to tissue mineralisation (a process

847   described by Sire 1993 in the scales of the armoured catfish *Corydoras arcuatus*).

848   The data above allow the identification of the site of basal bone formation of

849   mongolepid scales within the deep tiers of the corium, with the tissue being

850   considered to periodically increase in size due to the growth increments documented

851   in sectioned specimens. These depositional phases reveal a common pattern of

852   generation of mongolepid scale bases, wherein each newly laid down lamella covers

853   the lower surface of the previously deposited one. The geometry of the lamellae

854   shows little change, implying retention of a fairly consistent base shape throughout

855   scale ontogeny. Such a pattern of base morphogenesis is not unique to the

856   Mongolepidida, but appears to be the prevalent mode of bone tissue growth in the

857   scales of jawed gnathostomes, being demonstrated in 'placoderms' (Burrow & Turner,

858   1998, 1999), 'acanthodians' (Denison, 1979), early osteichthyans (Gross, 1968;

859   Schultze, 1968) and early chondrichthyans (Karatajūtė-Talimaa, 1973; Mader, 1986;

860   Wang, 1993).

861   **Canal system of mongolepid scales**

862   Previously, the internal canal system architecture of mongolepid scales had been

863   investigated in detail only in *Mongolepis*, *Teslepis* and *Sodolepis* through oil

864   immersion studies and thin section work (Karatajūtė-Talimaa et al., 1990; Karatajūtė-

865   Talimaa & Novitskaya, 1992, 1997). The employment of X-ray microtomography

866   extended to these observations by enabling visualization of the three-dimensional

867   structure of scale cavity spaces in the examined genera with greater accuracy.

868   In *Mongolepis*, *Teslepis*, *Sodolepis* and *Solinalepis* gen. nov. the lower ends of

869   odontode pulp cavities are continuous with the canal system of the base. Comparable

870   vascularization is developed in the Upper Ordovician chondrichthyan scale species

871   *Tezakia hardingensis* from North America (Andreev et al. 2015). The lower base

872   surface of this taxon has been demonstrated to exhibit rows of foramina (Sansom,

873   Smith & Smith, 1996, fig. 2a) that are similar to the basal canal openings of

874   mongolepids. Likewise, the central canal of the basal bone tissue is continuous with

875   the odontode pulp in the Silurian scale genera *Elegestolepis* (Karatajūtė-Talimaa,

876   1973; Andreev et al., in press) and *Kannathalepis* (Märss & Gagnier, 2001), which

877   are the earliest recorded monodontode scale taxa attributed to the Chondrichthyes

878   (Andreev et al., in press). This condition is also identified in the monodontode scales

879   of various Upper Palaeozoic chondrichthyans (e.g. *Janassa* Ørvig, 1966; Malzahn,

880   1968, *Ornithoprion* Zangerl, 1966 and *Hopleacanthus* Schaumberg, 1982), Mesozoic

881   hybodonts (Reif, 1978) and extant neoselachians (Reif, 1980; Miyake et al., 1999;

882   Johanson et al., 2008).

883   *Xinjiangichthys*, *Shiqianolepis* and *Rongolepis* differ from the other mongolepid

884   genera in having their entire scale canal system confined to the crown, with the lower

885   ends of odontode pulps opening at the crown surface in proximity of the base. The

886   posterior peripheral odontodes of these three genera display additional cavities that

887   are detected as foramina on the lower crown face. A similarly pitted lower crown

888   surface has also been identified in poracanthodid 'acanthodians' (Gross 1956;

889   Valiukevičius, 1992; Burrow, 2003), the putative stem chondrichthyan *Seretolepis*

890   (Hanke & Wilson, 2010; Martínez-Pérez et al., 2010), and in ctenacanthiform scales

891 (e.g. *Tamiobatis vetustus* Williams, 1998 and *Ctenacanthus costellatus* Reif, 1978). In

892 the scales of *Poracanthodes* these openings represent the posterior exit points of a

893 complex canal network that is absent from mongolepid scale crowns.

894   Studies on the squamation of jawed gnathostomes reveal the lack of basal

895 tissue vascularisation to be a common feature of many 'acanthodians' (Denison, 1979;

896 Karatajūtė-Talimaa & Smith, 2003; Valiukevičius, 2003; Valiukevičius & Burrow, 2005)

897 and euchondrichthyans such as *Protacrodus* (Gross, 1973), *Orodus* (Zangerl, 1968)

898 and *Holmesella* (Ørvig, 1966), including some of the earliest known post-Silurian

899 putative chondrichthyan taxa (e.g. *Iberolepis* and *Lunalepis* Mader, 1986;

900 *Nogueralepis* Wang, 1993; *Gladbachus* Burrow & Turner, 2013).

901   Despite the observed differences in canal architecture, all mongolepid genera

902 with the exception of *Sodolepis* develop canal openings exposed on the scale surface

903 in the region the crown-base interface. These foramina represent the termini of canals

904 that are positionally equivalent to, and likely homologues of, the neck canals of

905 euselachians (*sensu* Reif, 1978). In *Mongolepis* and *Teslepis* this connection is

906 established via one pair of short canals (the 'horizontal canals' of Karatajūtė-Talimaa

907 et al., 1990, Karatajūtė-Talimaa & Novitskaya, 1992 and Karatajūtė-Talimaa, 1998)

908 that emerge from the lower end of each pulp. The data presented here indicate that

909 the horizontal canal system of these two genera is housed inside the scale crown,

910 contrary to previous depictions of the feature at the crown-base junction (Karatajūtė-

911 Talimaa, 1995, 1998). In contrast, the lower ends of odontode pulp canals of North

912 American and Chinese mongolepids do not branch out, and either continue inside the

913 base without being exposed on the crown surface (*Solinalepis* gen. nov.) or open

914   directly onto it (*Shiqianolepis* and *Rongolepis*). These features point to notable

915   variation in the vascularization of mongolepid species, which are otherwise remarkably

916   consistent in the development of their scales. However, it is unclear if these

917   differences had any influence on the rates of growth and regeneration of the

918   integumentary skeleton.

919   **Systematic position of the Mongolepidida**

920   Recent phylogenetic investigations of Palaeozoic gnathostomes use only a small

921   subset of generalized scale characters (Brazeau, 2009; Davis, Finarelli & Coates,

922   2012; Zhu et al., 2013; Giles, Friedman & Brazeau, 2015), and this is likewise true for

923   tree reconstructions of the total group Chondrichthyes, where scale data tend to be

924   minor components of employed character matrices (Lund & Grogan, 1997; Coates &

925   Sequeira, 2001; Grogan & Lund, 2008; Grogan, Lund & Greenfest-Allen, 2012).

926   Chondrichthyan clades instead have often been erected upon tooth characters

927   (Zangerl, 1981; Stahl, 1999; Ginter, Hampe & Duffin, 2010), leaving the position of

928   lower Palaeozoic shark-like scale taxa still unresolved in phylogenetic hypotheses for

929   the Chondrichthyes.

930   The coherence of the Mongolepidida is reaffirmed here on the basis of an

931   amended character set, which diagnoses the Order by the unique combination of

932   scale growth, polyodontocomplex scale crowns and development of lamellin. The

933   placement of mongolepids within Chondrichthyes, on the other hand, has been

934   questioned in the past on the basis of their atubular dentine (lamellin) crowns and the

935   presence of a horizontal canal system (Karatajūtė-Talimaa & Novitskaya, 1992). This

936   study suggests that the horizontal canals of *Mongolepis* and *Teslepis* are equivalent to

937   euselachian neck canals, whilst revealing similar canal spaces in the crown odontodes

938   of Chinese mongolepids. However, neck canals are likewise also known in the scales

939   of 'placoderms' (Burrow & Turner, 1998) and basal Palaeozoic osteichthyans (Gross,

940   1953, 1968), and might not by a chondrichthyan apomorphy. Also, scale dentine

941   histology appears to vary greatly within the total group Chondrichthyes (e.g. distinct

942   dentine types are developed in *Elegestolepis* Karatajūtė-Talimaa, 1973, *Seretolepis*

943   Hanke and Wilson 2010, *Orodus* Zangerl, 1968 and *Hybodus* Reif, 1978), which

944   makes it a poor diagnostic character at a supra-ordinal level. By the same token,

945   although atubular dentine occurs in the Mongolepidida, it is also formed in the dermal

946   skeleton of some pteraspidomorph agnathans (Karatajūtė-Talimaa & Smith, 2004) and

947   fin spines that may be of chondrichthyan origin (Zhu, 1998; Sansom et al., 2005), and

948   therefore is uninformative with respect to the relationships of the Order. The

949   systematic affinities of Mongolepidida are determined instead by a unique combination

950   of scale attributes that are shared with other Palaeozoic chondrichthyan lineages.

951   Reference is made here to the *Ctenacanthus*-type squamation of certain

952   xenacanthiform (*Diplodoselache* Dick, 1981), orodontiform (*Orodus* Zangerl, 1968)

953   and cladodontomorph (e.g. *Cladolepis* Burrow, Turner & Wang, 2000 and

954   *Cladoselache* Dean, 1909; P. Andreev pers. obs.) chondrichthyans, characterized by

955   the development of symmetrical trunk scales with multiple crown odontocomplexes

956   that lack cancellous bone, enamel and hard tissue resorption.

957

958   CONCLUSIONS

959   The present revision of Mongolepidida established the Order as a natural group of

960   early chondrichthyans characterized by polyodontocomplex growing scales with

961   *Ctenacanthus*-like crown architecture. However, in agreement with Karatajūtė-Talimaa

962   (1992), the scales of mongolepids are recognized to exhibit a distinct, *Mongolepis*,

963   type of morphogenesis, on account of their lamellin composed crowns.

964   The description of the mongolepid genus *Solinalepis* gen. nov. from the

965   Sandbian of North America, pushes back the first appearance of the Mongolepidida by

966   20 My and places the origin of the Chondrichthyes in the Ordovician. Together with

967   reports of other shark-like scale taxa from the Ordovician (Sansom, Smith & Smith,

968   1996; Sansom, Smith & Smith, 2001; Sansom et al., 2012) and the Silurian

969   (Karatajūtė-Talimaa, 1973; Karatajūtė-Talimaa & Predtechenskyj, 1995; Sennikov et

970   al., 2015), this lends further support of an early diversification of putative

971   chondrichthyans (proposed by Karatajūtė-Talimaa, 1992) that preceded a major

972   radiation of nektonic faunas (Klug et al., 2010), coincident with the first known

973   appearance of chondrichthyan teeth and articulated skeletal remains in the Lower

974   Devonian.

975

976

977

978

979

980

981

982

983

984

ACKNOWLEDGEMENTS

Solinalepis material was collected from the Harding Sandstone during fieldwork
undertaken as part of research conducted by M. Paul Smith (Oxford) and Moya Smith
(King's College, London), and we are grateful to both for discussions on the nature of
these specimens over the years, whilst specimens of *Shiqianolepis* were made
available for study by the late Richard J. Aldridge (Leicester). Rachel Sammons and
Michael Sandholzer provided technical assistance during SEM and micro-CT imaging
of mongolepid scales at the School of Dentistry, University of Birmingham. We are
also grateful to Kate Trinajstic, Živilė Žigaitė and one anonymous reviewer for their
constructive and helpful comments on the originally submitted manuscript.

995 The authors would like to highlight the contribution of the deceased N-Z Wang to this

996 study, who initially examined and provided the Chinese mongolepid material described

997 here.

998

999

1000

1001

1002

1003

1004

1005 REFERENCES

1006 **Allard B, Magloire H, Couble ML, Maurin JC, Bleicher F. 2006**. Voltage-gated

1007 Sodium Channels Confer Excitability to Human Odontoblasts. *Journal of Biological*

1008 *Chemistry* **281**:29002–29010.

1009 **Andreev PS, Coates MI, Shelton RM, Cooper PR, Smith MP, Sansom IJ. 2015**.

1010 Upper Ordovician chondrichthyan-like scales from North America. *Palaeontology*

1011 **58**:691–704.

1012 **Andreev PS, Coates MI, Karatajūtė-Talimaa V, Shelton RM, Cooper PR, Sansom IJ.**

1013 **in press**. *Elegestolepis* and its kin, the earliest monodontode chondrichthyans. *Journal*

1014 *of Vertebrate Paleontology*.

1015 **Bolshakova L, Ulitina L. 1985.** Stromatoporates and biostratigraphy of the Lower

1016 Paleozoic in Mongolia. *Transsec. Joint Soviet–Mongolian paleontological expedition*

1017 **27**:1–94.

1018 **Botella H, Donoghue P, Martínez-Pérez C. 2009.** Enameloid microstructure in the

1019 oldest known chondrichthyan teeth. *Acta Zoologica* **90**:103–108.

1020 **Brazeau MD. 2009.** The braincase and jaws of a Devonian 'acanthodian' and modern

1021 gnathostome origins. *Nature* **457**:305–308.

1022 **Brazeau MD. 2012.** A revision of the anatomy of the Early Devonian jawed vertebrate

1023 *Ptomacanthus anglicus* Miles. *Palaeontology* **55**:355–367.

1024 **Brazeau MD, Friedman M. 2015.** The origin and early phylogenetic history of jawed

1025 vertebrates. *Nature* 520:490-497.

1026 **Burrow CJ. 2003.** Redescription of the gnathostome fish fauna from the mid-

1027 Palaeozoic Silverband Formation, the Grampians, Victoria. *Alcheringa* **27**:37–49.

1028 **Burrow CJ, Turner S. 1998.** Devonian placoderm scales from Australia. *Journal of*

1029 *Vertebrate Paleontology* **18**:677–695.

1030 **Burrow CJ, Turner S. 1999.** A review of placoderm scales, and their significance in

1031 placoderm phylogeny. *Journal of Vertebrate Paleontology* **19**:204–219.

1032 **Burrow CJ, Turner S. 2013.** Scale structure of putative chondrichthyan *Gladbachus*

1033 *adentatus* Heidtke & Krätschmer, 2001 from the Middle Devonian Rheinisches

1034 Schiefergebirge, Germany. *Historical Biology* **25**:385-390.

1035 **Burrow CJ, Turner S, Wang S. 2000.** Devonian microvertebrates from Longmenshan,

1036 China: Taxonomic assesssment. In: Blieck A, and Turner S, eds. *Palaeozoic vertebrate*

1037   *biochronology and global marine/non-marine correlation: final report of IGCP 328 (1991-*

1038   *1996)*. Frankfurt a. M.: Courier Forschungsinstitut Senckenberg, 391–451.

1039   **Coates M, Sequeira S. 2001.** A new stethacanthid chondrichthyan from the Lower

1040   Carboniferous of Bearsden, Scotland. *Journal of Vertebrate Paleontology* 21:438-459.

1041   **Davis SP, Finarelli JA, Coates MI. 2012.** *Acanthodes* and shark-like conditions in the

1042   last common ancestor of modern gnathostomes. *Nature* **486**:247–250.

1043   **Dean B. 1909.** Studies on fossil fishes (sharks, chimaeroids and arthrodires). *Memoirs*

1044   *of the American Museum of Natural History* **9**:211–248.

1045   **Denison RH. 1979.** *Acanthodii*. Stuttgart, New York: Gustav Fischer Verlag.

1046   **Dick JR. 1981.** *Diplodoselache woodi* gen. et sp. nov., an early Carboniferous shark

1047   from the Midland Valley of Scotland. *Transactions of the Royal Society of Edinburgh:*

1048   *Earth Sciences* **72**:99–113.

1049   **Dong XIP, Donoghue PCJ, Repetski JE. 2005.** Basal tissue structure in the earliest

1050   euconodonts: Testing hypotheses of developmental plasticity in euconodont phylogeny.

1051   *Palaeontology* **48**:411–421.

1052   **Donoghue PCJ. 1998.** Growth and patterning in the conodont skeleton. *Philosophical*

1053   *Transactions of the Royal Society B: Biological Sciences* **353**:633–666.

1054   **Donoghue PCJ, Sansom IJ. 2002.** Origin and early evolution of vertebrate

1055   skeletonization. *Microscopy research and technique* **59**:352–372.

1056   **Donoghue PCJ, Sansom IJ, Downs JP. 2006.** Early evolution of vertebrate skeletal

1057   tissues and cellular interactions, and the canalization of skeletal development. *Journal*

1058   *of Experimental Zoology Part B: Molecular and Developmental Evolution* **306**:278–294.

1059   **Downs JP, and Donoghue PC. 2009.** Skeletal histology of *Bothriolepis canadensis*

1060 (Placodermi, Antiarchi) and evolution of the skeleton at the origin of jawed vertebrates.

1061 *Journal of Morphology* **270**:1364–1380.

1062 **Gemballa S, Bartsch P. 2002.** Architecture of the integument in lower teleostomes:

1063 Functional morphology and evolutionary implications. *Journal of Morphology* **253**:290–

1064 309.

1065 **Giles S, Friedman M, and Brazeau MD. 2015.** Osteichthyan-like cranial conditions in

1066 an Early Devonian stem gnathostome. *Nature* **520**:82–85.

1067 **Ginter M, Hampe O, Duffin CJ. 2010.** *Chondrichthyes: Paleozoic Elasmobranchii:*

1068 *Teeth*. Munich: Verlag Dr. Friendrich Pfeil.

1069 **Goloboff PA, Farris JS, and Nixon KC. 2008.** TNT, a free program for phylogenetic

1070 analysis. *Cladistics* **24**:774-786.

1071 **Grogan ED, Lund R. 2008.** A basal elasmobranch, *Thrinacoselache gracia* n. gen and

1072 sp., (Thrinacodontidae, new family) from the Bear Gulch Limestone, Serpukhovian of

1073 Montana, USA. *Journal of Vertebrate Paleontology* **28**:970–988.

1074 **Grogan ED, Lund R, Greenfest-Allen E. 2012.** The origin and relationships of early

1075 chondrichthyans. In: Carrier JC, Musick J. A., Heithaus M. R., ed. *Biology of sharks and*

1076 *their relatives*. Boca Raton, FL: Taylor & Francis Inc, 3–27.

1077 **Gross W. 1953.** Devonische Palaeonisciden-Reste in Mittel-und Osteuropa.

1078 *Paläontologische Zeitschrift* **27**:85–112.

1079 **Gross W. 1956.** Über Crossopterygier und Dipnoer aus dem baltischen Oberdevon im

1080 Zusammenhang einer vergleichenden Untersuchung des Porenkanalsystems

1081 paläozoischer Agnathen und Fische. *Kungliga Svenska vetenskapsakademiens*

1082 *handlingar* **5**:1–140.

1083 **Gross W. 1968.** Fragliche Actinopterygier-Schuppen aus dem Silur Gotlands. *Lethaia*

1084 **1**:184–218.

1085 **Gross W. 1973.** Kleinschuppen, Flossenstacheln und Zähne von Fischen aus

1086 europäischen und nordamerikanischen Bonebeds des Devons. *Palaeontographica*

1087 *Abteilung A* **142**:51–155.

1088 **Hanke GF, Davis SP. 2008.** Redescription of the acanthodian *Gladiobranchus probaton*

1089 Bernacsek & Dineley, 1977, and comments on diplacanthid relationships. *Geodiversitas*

1090 **30**:303–330.

1091 **Hanke GF, Wilson MVH. 2004.** New teleostome fishes and acanthodian systematics.

1092 In: Arratia G, Wilson, M. V. H. & R. Cloutier ed. *Recent Advances in the Origin and*

1093 *Early Radiation of Vertebrates*. Munich: Verlag Dr. Friedrich Pfeil, 189–216.

1094 **Hanke GF, Wilson MVH. 2010.** The putative stem-group chondrichthyans

1095 *Kathemacanthus* and *Seretolepis* from the Lower Devonian MOTH locality, Mackenzie

1096 Mountains, Canada. In: D. K. Elliott JGM, X. Yu & D. Miao, ed. *Morphology, phylogeny*

1097 *and paleobiogeography of fossil fishes*. Munich: Verlag Dr. Friedrich Pfiel, 159–182.

1098 **Johanson Z, Smith MM, Joss JMP. 2007.** Early scale development in *Heterodontus*

1099 (Heterodontiformes; Chondrichthyes): a novel chondrichthyan scale pattern. *Acta*

1100 *Zoologica* **88**:249–256.

1101 **Johanson Z, Tanaka M, Chaplin N, Smith M. 2008.** Early Palaeozoic dentine and

1102 patterned scales in the embryonic catshark tail. *Biology letters* **4**:87–90.

1103 **Karatajūtė-Talimaa VN. 1973.** *Elegestolepis grossi* gen. et sp. nov., ein neuer Typ der

1104 Placoidschuppe aus dem Oberen Silur der Tuwa. *Palaeontographica Abt A* **143**:35–50.

1105 **Karatajūtė-Talimaa VN. 1992.** The early stages of the dermal skeleton formation in

1106   chondrichthyans. In: Mark-Kurik E, ed. *Fossil fishes as living animals*. Tallinn: Institute

1107   of Geology, 223–231.

1108   **Karatajūtė-Talimaa VN. 1995.** The Mongolepidida: scale structure and systematic

1109   position. *Geobios* **19**:35–37.

1110   **Karatajūtė-Talimaa VN. 1998.** Determination methods for the exoskeletal remains of

1111   early vertebrates. *Mitteilungen ausdem Museum für Naturkunde in Berlin,*

1112   *Geowissenschaftliche Reihe* **1**:21–51.

1113   **Karatajūtė-Talimaa VN, Novitskaya L. 1992.** *Teslepis*—a new representative of

1114   mongolepid elasmobranchs from the Lower Silurian of Mongolia. *Paleontologicheskii*

1115   *Zhurnal* **4**:36–46.

1116   **Karatajūtė-Talimaa VN, Novitskaya L. 1997.** *Sodolepis*—a new representative of

1117   Mongolepidida (Chondrichthyes?) from the Lower Silurian of Mongolia.

1118   *Paleontologicheskii Zhurnal* **5**:96–103.

1119   **Karatajūtė-Talimaa VN, Novitskaya L, Rozman KS, Sodov Z. 1990.** *Mongolepis*—a

1120   new lower Silurian genus of elasmobranchs from Mongolia. *Paleontologicheskii Zhurnal*

1121   **1**:76–86.

1122   **Karatajūtė-Talimaa V, Predtechenskyj N. 1995.** The distribution of the vertebrates in

1123   the Late Ordovician and Early Silurian palaeobasins of the Siberian Platform. *Bulletin du*

1124   *Muséum National d'Histoire Naturelle* 17:39-55.

1125   **Karatajūtė-Talimaa VN, Smith MM. 2003.** Early acanthodians from the Lower Silurian

1126   of Asia. *Transactions of the Royal Society of Edinburgh: Earth Sciences* **93**:277–299.

1127   **Karatajūtė-Talimaa VN, Smith MM. 2004.** *Tesakoviaspis concentrica*: microskeletal

1128   remains of a new order of vertebrate from the Upper Ordovician and Lower Silurian of

1129   Siberia. In: G. Arratia MVHWRC, ed. *Recent Advances in the Origin and Early Radiation*

1130   *of Vertebrates*. Munich, Germany: Verlag Dr. Friedrich Pfeil, 53–64.

1131   **Kerr T. 1952.** The scales of primitive living actinopterygians. *Proceedings of the*

1132   *Zoological Society of London* **122**:55–78.

1133   **Kerr T. 1955.** The scales of modern lungfish. *Proceedings of the Zoological Society of*

1134   *London* **125**:335–345.

1135   **Klug C, Kroeger B, Kiessling W, Mullins GL, Servais T, Frýda J, Korn D, Turner S.**

1136   **2010.** The Devonian nekton revolution. *Lethaia* **43**:465-477.

1137   **Linde A. 1989.** Dentin matrix proteins: composition and possible functions in

1138   calcification. *The Anatomical Record* **224**:154–166.

1139   **Linde A, Lundgren T. 1995.** From serum to the mineral phase. The role of the

1140   odontoblast in calcium transport and mineral formation. *International Journal of*

1141   *Developmental Biology* **39**:213–213.

1142   **Lund R, Grogan ED. 1997.** Relationships of the Chimaeriformes and the basal

1143   radiation of the Chondrichthyes. *Reviews in Fish Biology and Fisheries* **7**:65–123.

1144   **Mader H. 1986.** *Schuppen und Zähne von Acanthodiern und Elasmobranchiern aus*

1145   *dem Unter-Devon Spaniens (Pisces)*. Göttingen: Geologischen Institute der Georg-

1146   August-Universität Göttingen.

1147   **Magloire H, Couble ML, Romeas A, Bleicher F. 2004.** Odontoblast primary cilia: facts

1148   and hypotheses. *Cell biology international* **28**:93–99.

1149   **Magloire H, Couble ML, Thivichon-Prince B, Maurin JC, Bleicher F. 2009.**

1150   Odontoblast: a mechano-sensory cell. *Journal of Experimental Zoology Part B:*

1151   *Molecular and Developmental Evolution* **312**:416–424.

1152   **Maisey J, Miller R, Turner S. 2009.** The braincase of the chondrichthyan *Doliodus* from

1153   the Lower Devonian Campbellton formation of New Brunswick, Canada. *Acta Zoologica*

1154   **90**:109–122.

1155   **Malzahn E. 1968.** Über neue Funde von *Janassa bituminosa* (Schloth.) im

1156   niederrheinischen Zechstein. *Geologisches Jahrbuch* **85**:67–96.

1157   **Märss T, Gagnier PY. 2001.** A new chondrichthyan from the Wenlock, Lower Silurian,

1158   of Baillie-Hamilton Island, the Canadian Arctic. *Journal of Vertebrate Paleontology*

1159   **21**:693–701.

1160   **Martínez-Pèrez C, Dupret V, Manzanares E, Botella H. 2010.** New data on the Lower

1161   Devonian chondrichthyan fauna from Celtiberia (Spain). *Journal of Vertebrate*

1162   *Paleontology* **30**:1622–1627.

1163   **Miles RS. 1973.** Articulated acanthodian fishes from the Old Red Sandstone of

1164   England, with a review of the structure and evolution of the acanthodian shoulder-girdle.

1165   *Bulletin of the British Museum (Natural History)* **24**:111–213.

1166   **Miller RF, Cloutier R, Turner S. 2003.** The oldest articulated chondrichthyan from the

1167   Early Devonian period. *Nature* **425**:501–504.

1168   **Miyake T, Vaglia JL, Taylor LH, Hall BK. 1999.** Development of dermal denticles in

1169   skates (Chondrichthyes, Batoidea): patterning and cellular differentiation. *Journal of*

1170   *Morphology* **241**:61–81.

1171   **Motta P. 1977.** Anatomy and functional morphology of dermal collagen fibers in sharks.

1172   *Copeia*:454–464.

1173   **Murdock DJ, Dong X-P, Repetski JE, Marone F, Stampanoni M, Donoghue PC.**

1174   **2013.** The origin of conodonts and of vertebrate mineralized skeletons. *Nature* **502**:546–

1175 549.

1176 **Okumura R, Shima K, Muramatsu T, Nakagawa K, Shimono M, Suzuki T, Magloire**

1177 **H, Shibukawa Y. 2005.** The odontoblast as a sensory receptor cell? The expression of

1178 TRPV1 (VR-1) channels. *Archives of histology and cytology* **68**:251–257.

1179 **Ørvig T. 1951.** Histologic studies of Placoderms and fossil Elasmobranchs I: The

1180 endoskeleton, with remarks on the hard tissues of lower vertebrates in general. *Arkiv för*

1181 *Zoologie* 2:321-456.

1182 **Ørvig T. 1966.** Histologic studies of ostracoderms, placoderms and fossil

1183 elasmobranchs. 2. On the dermal skeleton of two late Palaeozoic Elasmobranchs. *Arkiv*

1184 *för Zoologi* **19**:1–39.

1185 **Ørvig T. 1968.** The dermal skeleton: general considerations. In: Ørvig T, ed. *Current*

1186 *problems of lower vertebrate phylogeny*. Stockholm: Almquist and Wiksell, 374–397.

1187 **Ørvig T. 1977.** A survey of odontodes ('dermal teeth') from developmental, structural,

1188 functional, and phyletic points of view. In: Andrews M, R. S. & Walker, A. D., ed.

1189 *Problems in Vertebrate Evolution*. London, New York: Academic Press, 53–75.

1190 **Pradel A, Maisey JG, Tafforeau P, Mapes RH, Mallatt J. 2014.** A Palaeozoic shark

1191 with osteichthyan-like branchial arches. *Nature* 509:608–611.

1192 **Reif WE. 1978.** Types of morphogenesis of the dermal skeleton in fossil sharks.

1193 *Paläontologische Zeitschrift* **52**:110–128.

1194 **Reif WE. 1980.** Development of dentition and dermal skeleton in embryonic

1195 *Scyliorhinus canicula*. *Journal of Morphology* **166**:275–288.

1196 **Sansom IJ. 1996.** *Pseudooneotodus*: a histological study of an Ordovician to Devonian

1197 vertebrate lineage. *Zoological Journal of the Linnean Society* **118**:47–57.

1198   **Sansom IJ, Aldridge R, Smith M. 2000.** A microvertebrate fauna from the Llandovery

1199   of South China. *Transactions of the Royal Society of Edinburgh: Earth Sciences*

1200   **90**:255–272.

1201   **Sansom IJ, Davies NS, Coates MI, Nicoll RS, Ritchie A. 2012.** Chondrichthyan-like

1202   scales from the Middle Ordovician of Australia. *Palaeontology* **55**:243–247.

1203   **Sansom IJ, Smith MM, Smith MP. 1996.** Scales of thelodont and shark-like fishes from

1204   the Ordovician of Colorado. *Nature* **379**:628–630.

1205   **Sansom IJ, Smith MM, Smith MP. 2001.** The Ordovician radiation of vertebrates. In:

1206   Ahlberg E, ed. *Major Events in Early Vertebrate Evolution, Systematics Association*

1207   *Special Volume*. London and New York: Taylor & Francis, 156–171.

1208   **Sansom IJ, Wang NZ, Smith M. 2005.** The histology and affinities of sinacanthid

1209   fishes: primitive gnathostomes from the Silurian of China. *Zoological Journal of the*

1210   *Linnean Society* **144**:379–386.

1211   **Sasagawa I. 1995.** Evidence of two types of odontoblasts during dentinogenesis in

1212   Elasmobranchs. *Connective tissue research* **33**:223–229.

1213   **Schaumberg G. 1982.** *Hopleacanthus richelsdorfensis* n. g. n. sp., ein Euselachier aus

1214   dem permischen Kupferschiefer von Hessen (W-Deutschland). *Paläontologische*

1215   *Zeitschrift* **56**:235–257.

1216   **Schmidt WJ, Keil A. 1971.** *Polarizing microscopy of dental tissues*: Pergamon Press.

1217   **Schultze H-P. 1968.** Palaeoniscoidea-Schuppen aus dem Unterdevon Australiens und

1218   Kanadas und aus dem Mitteldevon Spitzbergens. *Bulletin of the British Museum*

1219   *(Natural History)* **16**:343–368.

1220   **Sennikov N, Rodina O, Izokh N, Obut O. 2015.** New data on Silurian vertebrates of

1221   southern Siberia. *Palaeoworld* **24**:231–242.

1222   **Servais T, Owen AW, Harper DA, Kröger B, Munnecke A. 2010.** The great ordovician

1223   biodiversification event (GOBE): the palaeoecological dimension. *Palaeogeography,*

1224   *Palaeoclimatology, Palaeoecology* **294**:99–119.

1225   **Sire JY. 1994.** Light and TEM study of nonregenerated and experimentally regenerated

1226   scales of *Lepisosteus oculatus* (Holostei) with particular attention to ganoine formation.

1227   *The Anatomical Record* **240**:189–207.

1228   **Sire JY. 2005.** Development and fine structure of the bony scutes in *Corydoras*

1229   *arcuatus* (Siluriformes, Callichthyidae). *Journal of Morphology* **215**:225–244.

1230   **Sire JY, Donoghue PCJ, Vickaryous MK. 2009.** Origin and evolution of the

1231   integumentary skeleton in non-tetrapod vertebrates. *Journal of anatomy* **214**:409–440.

1232   **Sire JY, Huysseune A. 1996.** Structure and development of the odontodes in an

1233   armoured catfish, *Corydoras aeneus* (Siluriformes, Callichthyidae). *Acta Zoologica*

1234   **77**:51–72.

1235   **Sire JY, Huysseune A. 2003.** Formation of dermal skeletal and dental tissues in fish: a

1236   comparative and evolutionary approach. *Biological Reviews* **78**:219–249.

1237   **Smith MM. 1979.** Scanning electron microscopy of odontodes in the scales of a

1238   coelacanth embryo, *Latimeria chalumnae* Smith. *Archives of oral biology* **24**:179–183.

1239   **Smith MM, Hall BK. 1993.** A developmental model for evolution of the vertebrate

1240   exoskeleton and teeth. *Evolutionary biology*: Springer, 387–448.

1241   **Smith MM, Hobdell MH, Miller W. 1972.** The structure of the scales of *Latimeria*

1242   *chalumnae*. *Journal of Zoology* **167**:501–509.

1243   **Smith MM, Sansom IJ, Smith MP. 1996.** 'Teeth' before armour: The earliest vertebrate

1244   mineralized issues. *Modern Geology* **20**:303–319.

1245   **Stahl BJ. 1999.** *Chondrichthyes III: Holocephali*. Munich: Verlag Dr. Friedrich Pfeil.

1246   **Stensiö E**. 1961. Permian vertebrates. In: Raasch G, ed. *Geology of the Arctic*.

1247   Toronto: University of Toronto, 231-247.

1248   **Thorsteinsson R. 1973.** Dermal elements of a new lower vertebrate from Middle

1249   Silurian (Upper Wenlockian) Rocks of the Canadian Arctic Archipelago.

1250   *Palaeontographica Abteilung A* **143**:51–57.

1251   **Turner S, Blieck A, Nowlan G. 2004.** Vertebrates (agnathans and gnathostomes). In:

1252   Webby BD, Paris F, Droser ML, and Percival I, eds. *The Great Ordovician*

1253   *Biodiversification Event*: Columbia University Press, 327–335.

1254   **Valiukevičius J. 1992.** First articulated *Poracanthodes* from the Lower Devonian of

1255   Severnaya Zemlya. In: Mark-Kurik E, ed. *Fossil Fishes as Living Animals*. Tallinn:

1256   Academy of Sciences of Estonia, 193–214.

1257   **Valiukevičius J. 2003.** Devonian acanthodians from Severnaya Zemlya Archipelago

1258   (Russia). *Geodiversitas* **25**:131–204.

1259   **Valiukevičius J, Burrow CJ. 2005.** Diversity of tissues in acanthodians with

1260   *Nostolepis*-type histological structure. *Acta Palaeontologica Polonica* **50**:635–649.

1261   **Wang N-Z, Zhang S-B, Wang J-Q, Zhu M. 1998.** Early Silurian chondrichthyan

1262   microfossils from Bachu County, Xinjiang, China. *Vertebrata PalAsiatica* **36**:257–267.

1263   **Wang R. 1993.** *Taxonomie, Palökologie und Biostratigraphie der Mikroichthyolithen aus*

1264   *dem Unterdevon Keltiberiens, Spanien*. Frankfurt a. M.: Senckenbergische

1265   Naturforschende Gesellschaft.

1266   **Webby BD, Paris F, Droser ML. 2004.** *The great Ordovician biodiversification event*.

New York: Columbia University Press.

Williams ME. 1998. A new specimen of *Tamiobatis vetustus* (Chondrichthyes, Ctenacanthoidea) from the late Devonian Cleveland Shale of Ohio. *Journal of Vertebrate Paleontology* **18**:251–260.

Yoshiba K, Yoshiba N, Ejiri S, Iwaku M, Ozawa H. 2002. Odontoblast processes in human dentin revealed by fluorescence labeling and transmission electron microscopy. *Histochemistry and cell biology* **118**:205–212.

Young G. 1982. Devonian sharks from south-eastern Australia and Antarctica. *Palaeontology* **25**:817–843.

Zangerl R. 1966. A new shark of the family Edestidae, *Ornithoprion hertwigi*, from the Pennslyvanian Mecca and Logan quarry shales of Indiana. *Fieldiana: Geology* **16**:1–43.

Zangerl R. 1968. The morphology and the developmental history of the scales of the Paleozoic sharks *Holmesella*? sp. and *Orodus*. In: Ørvig T, ed. *Current Problems of Lower Vertebrate Phylogeny*. Stockholm: Almqvist & Wiksell, 399–412.

Zangerl R. 1981. *Chondrichthyes I: Paleozoic Elasmobranchii*. Stuttgart and New York: Gustav Fischer.

Zeng XY. 1988. Some fin-spines of Acanthodii from Early Silurian of Hunan, China. *Vertebrata Palasiatica* **26**:287-295.

Zhu M. 1998. Early Silurian sinacanths (Chondrichthyes) from China. *Palaeontology* **41**:157–172.

Zhu M, Yu X, Ahlberg PE, Choo B, Lu J, Qiao T, Qu Q, Zhao W, Jia L, Blom H. 2013. A Silurian placoderm with osteichthyan-like marginal jaw bones. *Nature* **502**:188–193.

1290 **Žigaitė Ž. 2004.** A new thelodont from Lower Silurian of Tuva and north-west Mongolia.

1291 *Acta Universitatis Latviensis* 679:158–165.

1292 **Žigaitė Ž. 2013.** Endemic thelodonts (Vertebrata: Thelodonti) from the Lower Silurian of

1293 central Asia and southern Siberia. *Earth and Environmental Science Transactions of the*

1294 *Royal Society of Edinburgh* 104:123–143.

1295 **Žigaitė Ž, Karatajūtė-Talimaa V. 2008.** New genus of chondrichthyans from the

1296 Silurian–Devonian boundary deposits of Tuva (Russia). *Acta Geologica Polonica*

1297 58:127–131.

1298 **Žigaitė Ž, Karatajūtė-Talimaa V, Blieck A. 2011.** Vertebrate microremains from the

1299 Lower Silurian of Siberia and Central Asia: palaeobiodiversity and palaeobiogeography.

1300 *Journal of Micropalaeontology* **30**:97–106.

1301 **Zylberberg L, Géraudie J, Meunier F, and Sire J. 1992.** Biomineralization in the

1302 integumental skeleton of the living lower vertebrates. In: Hall BK, ed. *Bone: Vol. 4:*

1303 *bone metabolism and mineralization*: CRC Press Inc., 171-224.

1304

1305

1306

1307

1308

1309

1310

1311

1312

1313 **Figure captions**

1314 Figure 1 **Principle morphological features of scales.** Line drawing of a *Mongolepis*

1315 scale (BU5296) from the Chargat Formation of north-western Mongolia in lateral view.

1316 Figure 2 **Character distribution within Mongolepidida**. Cladogram based on a yet

1317 to be published scale-based phylogeny of early chondrichthyans by Andreev, Coates

1318 & Sansom (unpublished). Portion of a majority-rule consensus tree generated in TNT

1319 version 1.1 (Goloboff, Farris & Nixon, 2008) using a data matrix of 68 equally weighted

1320 scale-based characters (53 original and 15 revised/adopted) and 49 Palaeozoic

1321 jawed-gnathostome taxa.

1322 Figure 3 **Scale morphology of Mongolepididae.** (A–C) *Mongolepis rozmanae* scale

1323 BU5296 (Chargat Formation, north-western Mongolia) in (A) anterior (B) lateral, (C) and

1324 basal aspect and a *M. rozmanae* scale in (D) crown view (BU5351, Chargat Formation,

1325 north-western Mongolia); (E, G) *Teslepis jucunda* BU5322 (Chargat Formation, north-

1326 western Mongolia) in (E) crown and (G) basal view and a *T. jucunda* scale (BU5352,

1327 Chargat Formation, north-western Mongolia) in an (F) antero-lateral view; (H–J)

1328 *Sodolepis lucens* scales (Chargat Formation, north-western Mongolia) in (H) lateral

1329 (BU5305), crown (BU5304) and (J) basal (BU5355) views; (K–M) *Rongolepis cosmetica*

1330   scale BU5303 (Xiushan Formation, south China) in (K) crown, (L) lateral and (M) basal

1331   views;. Volume renderings, (A–C), (H) and (K–M); SEM micrographs, (D–G) and (I, J).

1332   Crown and base foramina indicated by arrows and arrowheads respectively. Anterior to

1333   the left in (B), (H), (L) and bottom in (A–G), (H–K), (M). Scale bar equals 500 μm in (D,

1334   I, J), 400 μm in (A–C), 300 μm in (H, K) and 200 μm in (E–G, L, M).

1335   Figure 4 **Scale morphology of Shiqianolepidae.** (A–C) *Shiqianolepis hollandi* scales

1336   (Xiushan Formation, south China) in (A) lateral (NIGP 130307), (B) crown (NIGP

1337   130309) and (C) postero-basal (NIGP 130307) views; (D–F) *Xinjiangichthys*

1338   *pluridentatus* scale IVPP V X2 (Yimugantawu Formation, north-western China) in (D)

1339   anterior, (E) posterior and (F) antero-lateral views. All images volume renderings except

1340   (B). Crown foramina indicated by arrows. Anterior to the left in (A), to the right in (F) and

1341   bottom in (B). Scale bar equals 300 μm in (A, B) and 200 μm in (C–F).

1342   Figure 5 **SEM micrographs of *Solinalepis levis* gen. et sp. nov. scales from the**

1343   **Upper Ordovician Harding Sandstone of Colorado, USA.** (A–C) tessera-like head

1344   scales in (A, B) crown (BU5307, BU5308) and (C) lateral (BU5309) views; (D) bulbous

1345   head scale (BU5312) in lateral view; (E–I) polygonal trunk scales, (E) holotype

1346   (BU5310) in anterior view, (F) BU5345 in crown, (G) corono-lateral and (H) partial

1347   posterior views, (I) BU5313 in basal view; J–L, lanceolate trunk scales in (J) anterior

1348   (BU5314), (K) lateral (BU5315) and (L) posterior (BU5311) views. Base foramina

1349   indicated by arrowheads. Anterior to the left in (G) and (K). Scale bar equals 300 μm

1350   in (A, B), 200 μm in (C), 100 μm in (D–G, I–L), and 50 μm in (H).

1351 Figure 6 **Scale histology of Mongolian and Chinese mongolepids.** (A) medial

1352 longitudinal section of a *Mongolepis rozmanae* scale (BU5297; Chargat Formation,

1353 north-western Mongolia); (B) detail of (A) depicting primary and secondary odontodes at

1354 the anterior crown margin; (C) primary odontode lamellin microstructure in a

1355 longitudinally sectioned *Mongolepis rozmanae* scale (BU5298; Chargat Formation,

1356 north-western Mongolia), etched for 10 min in 0.5% orthophosphoric acid; (D) basal

1357 bone microstructure of a longitudinally sectioned *Mongolepis rozmanae* scale (BU5354;

1358 Chargat Formation, north-western Mongolia) etched for 10 min in 0.5% orthophosphoric

1359 acid; (E) detail of BU5354 depicting the bone tissue of the anterior basal platform; (F)

1360 medial longitudinal section of a *Teslepis jucunda* scale (BU5324; Chargat Formation,

1361 north-western Mongolia); (G) lamellin architecture of two odontodes in a longitudinally

1362 sectioned *Sodolepis lucens* scale (BU5306; Chargat Formation, north-western

1363 Mongolia) etched for 10 min in 0.5% orthophosphoric acid; (H) basal bone

1364 microstructure in BU5306 at the anterior projection of the base; (I), sagittal longitudinal

1365 section of a *Sodolepis lucens* scale (BU5344; Chargat Formation, north-western

1366 Mongolia); (J) anterior third of BU5306 showing the contact between the globular crown

1367 dentine and the underlying basal bone; (K) sagittal longitudinal section of a *Rongolepis*

1368 *cosmetica* scale (NIGP 130328; Xiushan Formation, south China); (L) detail of NIGP

1369 130328 showing the mid third of the scale crown; (M) *Xinjiangichthys pluridentatus*

1370 scale (IVPP V X1; Yimugantawu Formation, north-western China) in longitudinal

1371 section; (N) sagittal longitudinal section of a *Shiqianolepis hollandi* trunk scale (NIGP

1372 130312; Xiushan Formation, south China). Nomarski differential interference contrast

1373 optics micrographs, (A), (B), (D), (F), (G), (I) and (K–N); SEM micrographs, (C), (E), (H)

1374 and (J). Anterior towards the left in (A–J, L) and towards the right in (K), (M) and (N).

1375 Abbreviations: gb, globular dentine; lb, lamellar bone; red dotted lines, contact surfaces

1376 between primary and secondary odontodes; white dotted lines, border between globular

1377 dentine and basal bone; white dashed line, contact surfaces between primary

1378 odontodes in *Rongolepis*. Asterisks mark bone layers with fibre orientation parallel to

1379 the section axis. Scale bar equals 400 µm in (A), 100 µm in (B, G, H, M), 20 µm in (C),

1380 200 µm in (D, F, K, N), 50 µm in (E, J, L), and 300 µm in (I).

1381 Figure 7 **Histology of *Solinalepis levis* gen. et sp. nov. scales.** (A) thin-sectioned

1382 head scale (BU5317) from the Harding Sandstone, Colorado, USA; (B) transverse

1383 section of a *Solinalepis levis* gen. et sp. nov. trunk scale (BU5316) from the Harding

1384 Sandstone, Colorado, USA. Scale bar equals 200 µm in (A) and 100 µm in (B).

1385 Figure 8 **Canal system of mongolepid scales.** Volume renderings. (A–C) canals (red)

1386 inside a translucent *Mongolepis rozmanae* scale (BU5296) in (A) lateral view, in (B)

1387 posterior view sliced along the plane 1 and in (C, C1) crown view sliced along plane 2;

1388 (D, D1) canals in a transversely sliced *Teslepis jucunda* scale (BU5325) shown in

1389 posterior view; (E) pulp cavities (red) in a transversely sliced *Sodolepis lucens* scale

1390 (BU5305) shown in postero-lateral view; (F) longitudinally sliced *Shiqianolepis hollandi*

1391 scale (NIGP 130307) in baso-lateral view; (G, H) longitudinally sliced *Xinjiangichthys*

1392 *pluridentatus* scale IVPP V X2 in (G) posterior and (H) lateral views; (I, J) canals system

1393 (red) inside a transversely sliced *Solinalepis levis* gen. et sp. nov. scale (BU5318)

1394 shown in posterior view, (J) detail of (I). Horizontal canals depicted in purple in c1 and

1395 d1. Yellow arrowheads point at canal openings on the sub-crown surface. Red dotted

1396 line, contact surfaces between primary and secondary odontodes; grey dotted line,

1397   crown/base border. Scale bar equals 400 µm in (A–C), 100 µm in (D, H, I), 200 µm in

1398   (E), 300 µm (F, G) and 50 µm in (J).

1399   Figure 9 **Odontocomplex organization of mongolepid scale crowns.** (A) *Teslepis*

1400   *jucunda* (BU5323) scale, medial portion of the crown; (B) *Shiqianolepis hollandi* (NIGP

1401   130309) scale, medial portion of the crown; (C) *Solinalepis levis* gen. et sp. nov. trunk

1402   scale (BU5314), lateral portion of the crown. Primary odontocomplex structure in

1403   Mongolepidida demonstrated by line drawings of longitudinally sectioned (D)

1404   *Mongolepis rozmanae* (BU5297) and (E) *Shiqianolepis hollandi* (NIGP 130312) scales.

1405   In (A–C) some of the odontocomplexes are highlighted in red and green. Dark green

1406   and dark red, odd numbered odontodes; light green and light red, even numbered

1407   odontodes. In (D, E)—light grey, primary odontodes; light yellow, secondary odontodes.

1408   Anterior towards the bottom in (A–C) and towards the left in (D, E). Scale bar equals

1409   100 µm in (A), 200 µm in (B) and 50 µm in (C).

1410

1411

1412

1

Principle morphological features of scales

Figure 1 **Principle morphological features of scales.** Line drawing of a *Mongolepis* scale (BU5296) from the Chargat Formation of north-western Mongolia in lateral view.
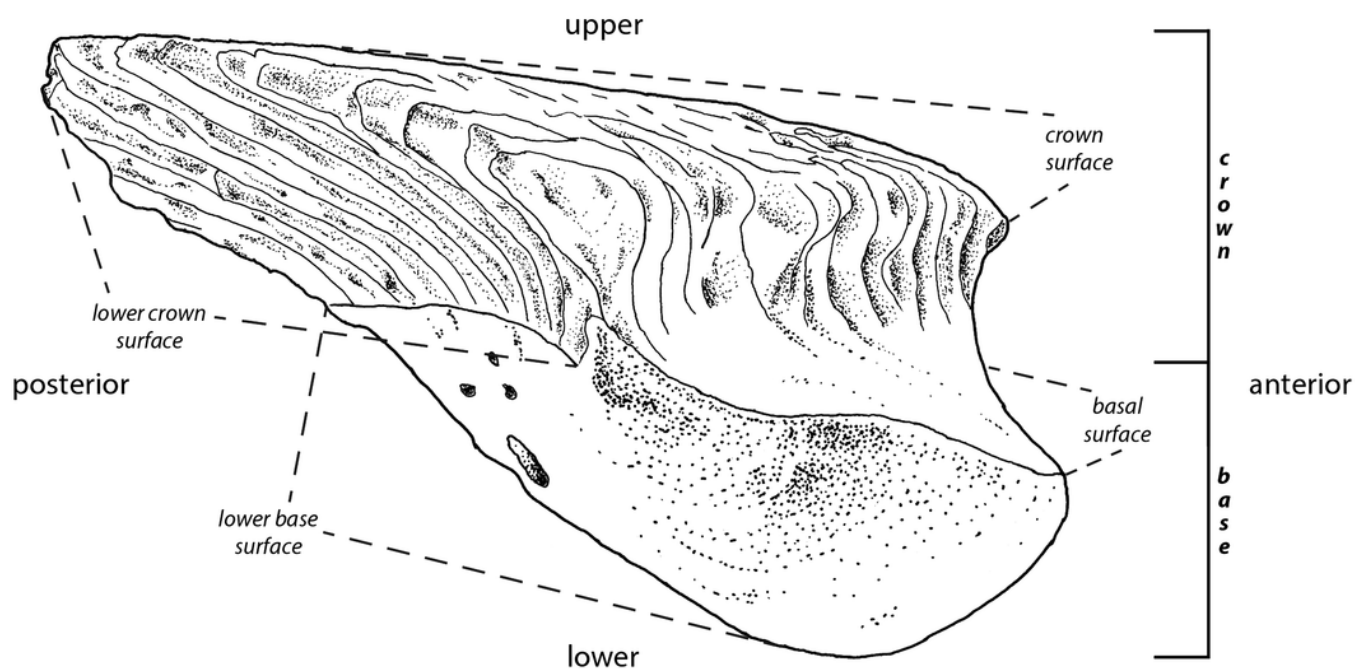
Character distribution within Mongolepidida

Figure 2 **Character distribution within Mongolepidida.** Cladogram based on a yet to be published scale-based phylogeny of early chondrichthyans by Andreev, Coates & Sansom (unpublished). Portion of a majority-rule consensus tree generated in TNT version 1.1 (Goloboff, Farris & Nixon, 2008) using a data matrix of 68 equally weighted scale-based characters (53 original and 15 revised/adopted) and 49 Palaeozoic jawed-gnathostome taxa.
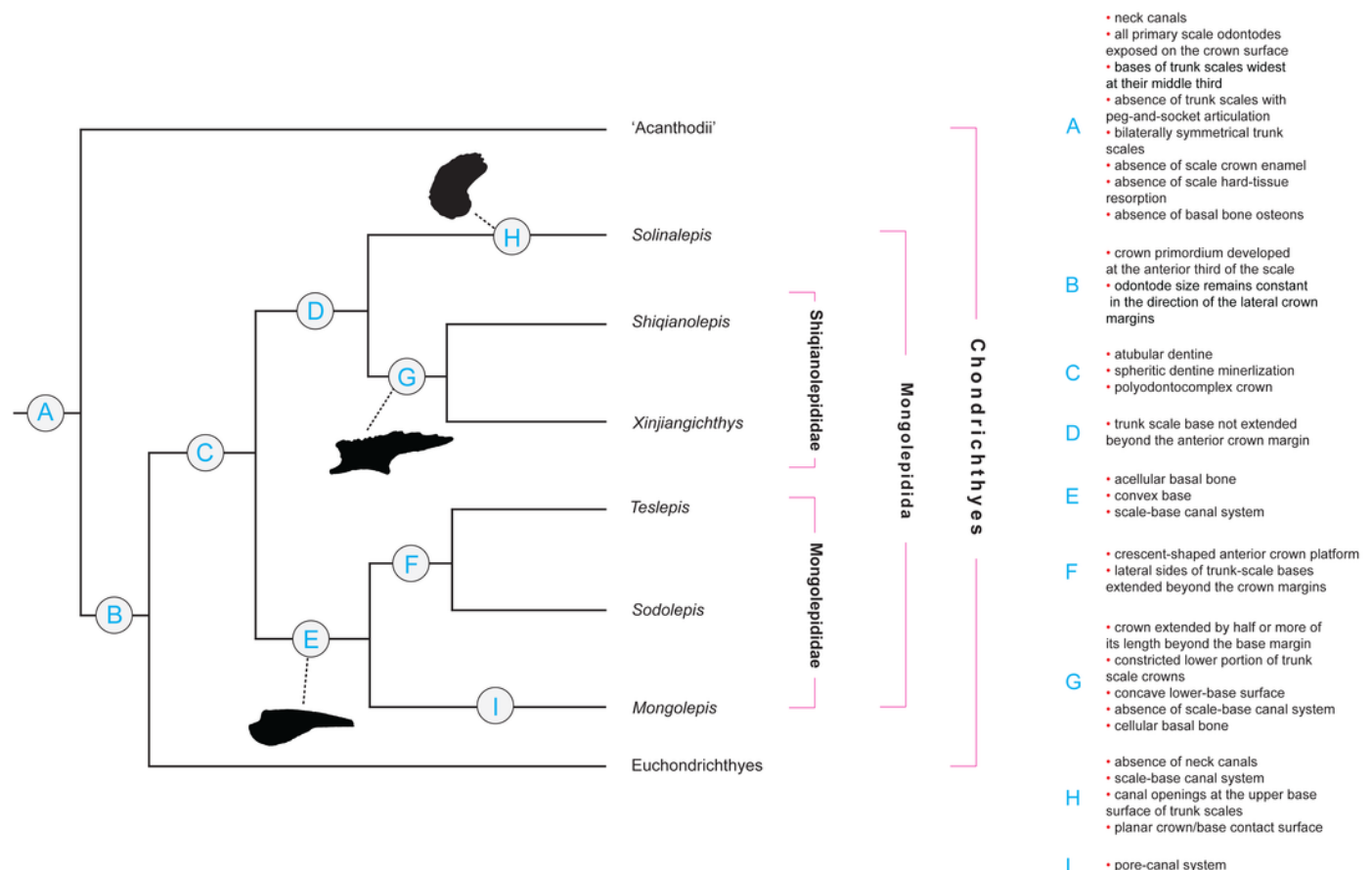
Scale morphology of Mongolepididae

Figure 3 **Scale morphology of Mongolepididae.** (A–C) *Mongolepis rozmanae* scale BU5296 (Chargat Formation, north-western Mongolia) in (A) anterior (B) lateral, (C) and basal aspect and a *M. rozmanae* scale in (D) crown view (BU5351, Chargat Formation, north-western Mongolia); (E, G) *Teslepis jucunda* BU5322 (Chargat Formation, north-western Mongolia) in (E) crown and (G) basal view and a *T. jucunda* scale (BU5352, Chargat Formation, north-western Mongolia) in an (F) antero-lateral view; (H–J) *Sodolepis lucens* scales (Chargat Formation, north-western Mongolia) in (H) lateral (BU5305), crown (BU5304) and (J) basal (BU5355) views; (K–M) *Rongolepis cosmetica* scale BU5303 (Xiushan Formation, south China) in (K) crown, (L) lateral and (M) basal views;. Volume renderings, (A–C), (H) and (K–M); SEM micrographs, (D–G) and (I, J). Crown and base foramina indicated by arrows and arrowheads respectively. Anterior to the left in (B), (H), (L) and bottom in (A–G), (H–K), (M). Scale bar equals 500 μm in (D, I, J), 400 μm in (A–C), 300 μm in (H, K) and 200 μm in (E–G, L, M).

Note: Auto Gamma Correction was used for the image. This only affects the reviewing manuscript. See original source image if needed for review.
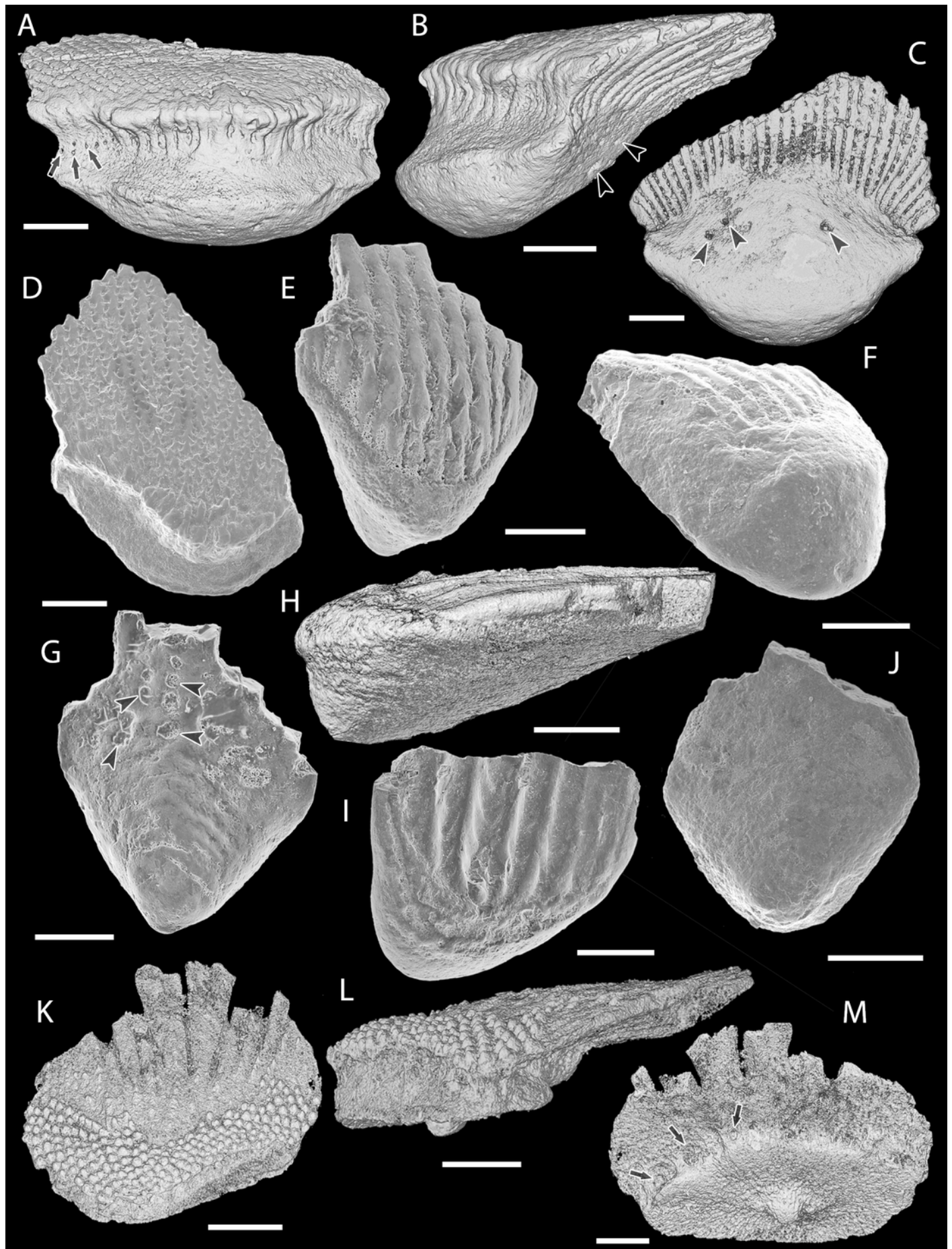
Scale morphology of Shiqianolepidae

Figure 4 **Scale morphology of Shiqianolepidae.** (A–C) *Shiqianolepis hollandi* scales (Xiushan Formation, south China) in (A) lateral (NIGP 130307), (B) crown (NIGP 130309) and (C) postero-basal (NIGP 130307) views; (D–F) *Xinjiangichthys pluridentatus* scale IVPP V X2 (Yimugantawu Formation, north-western China) in (D) anterior, (E) posterior and (F) antero-lateral views. All images volume renderings except (B). Crown foramina indicated by arrows. Anterior to the left in (A), to the right in (F) and bottom in (B). Scale bar equals 300 μm in (A, B) and 200 μm in (C–F).

Note: Auto Gamma Correction was used for the image. This only affects the reviewing manuscript. See original source image if needed for review.
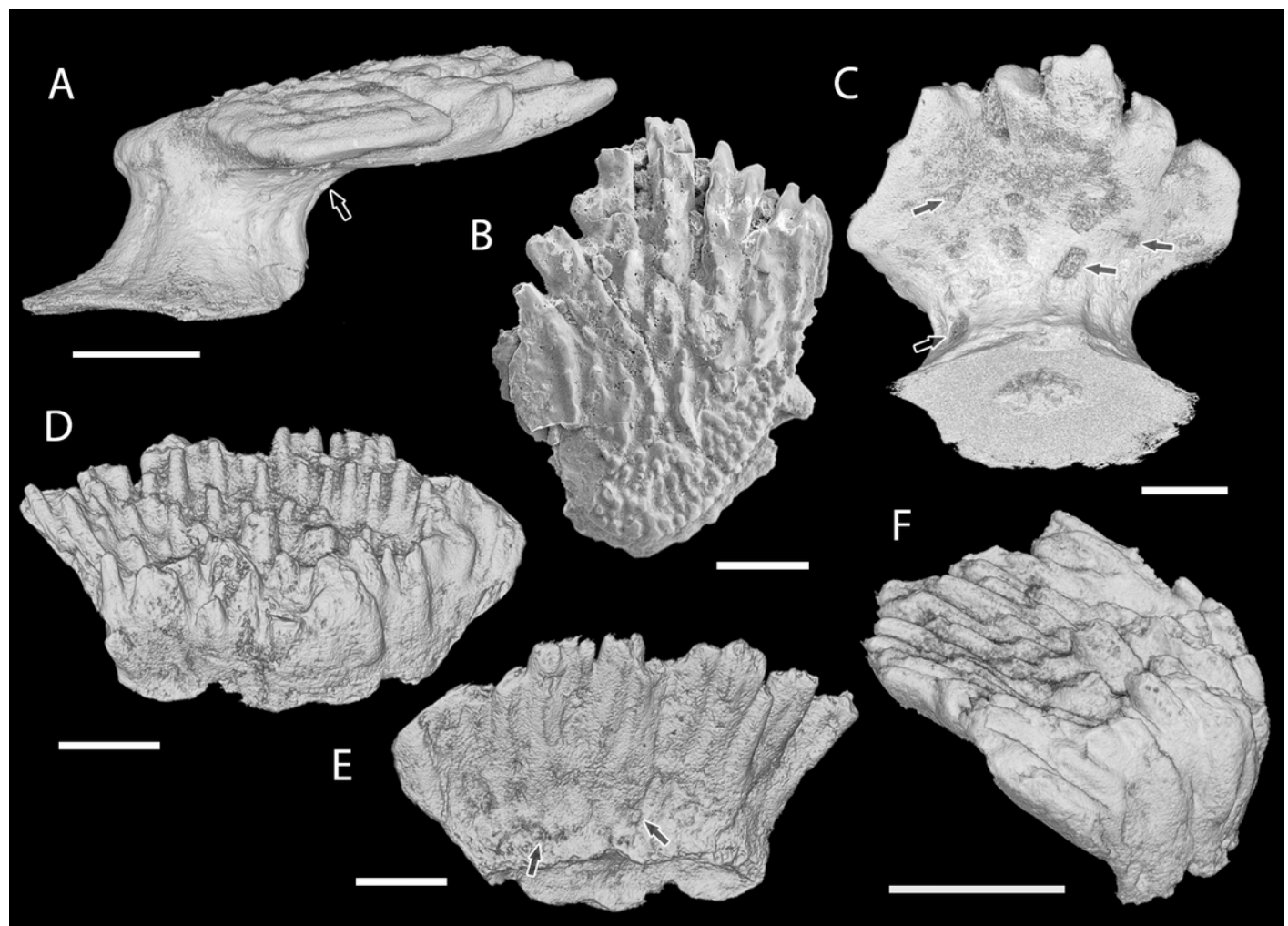
SEM micrographs of *Solinalepis levis* gen. et sp. nov. scales

Figure 5 **SEM micrographs of *Solinalepis levis* gen. et sp. nov. scales from the Upper Ordovician Harding Sandstone of Colorado, USA.** (A–C) tessera-like head scales in (A, B) crown (BU5307, BU5308) and (C) lateral (BU5309) views; (D) bulbous head scale (BU5312) in lateral view; (E–I) polygonal trunk scales, (E) holotype (BU5310) in anterior view, (F) BU5345 in crown, (G) corono-lateral and (H) partial posterior views, (I) BU5313 in basal view; J–L, lanceolate trunk scales in (J) anterior (BU5314), (K) lateral (BU5315) and (L) posterior (BU5311) views. Base foramina indicated by arrowheads. Anterior to the left in (G) and (K). Scale bar equals 300 µm in (A, B), 200 µm in (C), 100 µm in (D–G, I–L), and 50 µm in (H).

Note: Auto Gamma Correction was used for the image. This only affects the reviewing manuscript. See original source image if needed for review.

6
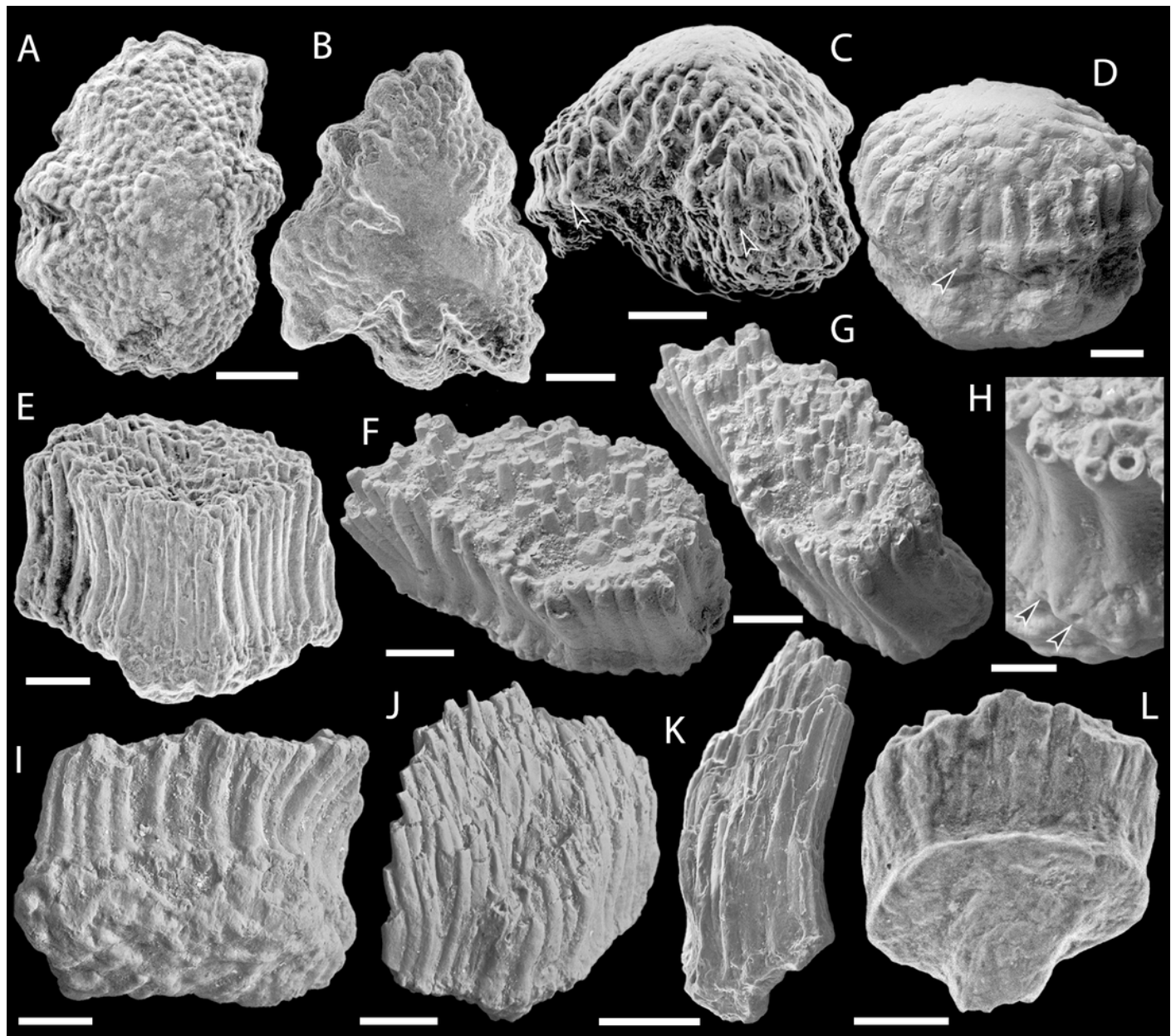
Scale histology of Mongolian and Chinese mongolepids

Figure 6 **Scale histology of Mongolian and Chinese mongolepids.** (A) medial longitudinal section of a *Mongolepis rozmanae* scale (BU5297; Chargat Formation, north-western Mongolia); (B) detail of (A) depicting primary and secondary odontodes at the anterior crown margin; (C) primary odontode lamellin microstructure in a longitudinally sectioned *Mongolepis rozmanae* scale (BU5298; Chargat Formation, north-western Mongolia), etched for 10 min in 0.5% orthophosphoric acid; (D) basal bone microstructure of a longitudinally sectioned *Mongolepis rozmanae* scale (BU5354; Chargat Formation, north-western Mongolia) etched for 10 min in 0.5% orthophosphoric acid; (E) detail of BU5354 depicting the bone tissue of the anterior basal platform; (F) medial longitudinal section of a *Teslepis jucunda* scale (BU5324; Chargat Formation, north-western Mongolia); (G) lamellin architecture of two odontodes in a longitudinally sectioned *Sodolepis lucens* scale (BU5306; Chargat Formation, north-western Mongolia) etched for 10 min in 0.5% orthophosphoric acid; (H) basal bone microstructure in BU5306 at the anterior projection of the base; (I), sagittal longitudinal section of a *Sodolepis lucens* scale (BU5344; Chargat Formation, north-western Mongolia); (J) anterior third of BU5306 showing the contact between the globular crown dentine and the underlying basal bone; (K) sagittal longitudinal section of a *Rongolepis cosmetica* scale (NIGP 130328; Xiushan Formation, south China); (L) detail of NIGP 130328 showing the mid third of the scale crown; (M) *Xinjiangichthys pluridentatus* scale (IVPP V X1; Yimugantawu Formation, north-western China) in longitudinal section; (N) sagittal longitudinal section of a *Shiqianolepis hollandi* trunk scale (NIGP 130312; Xiushan Formation, south China). Nomarski differential interference contrast optics micrographs, (A), (B), (D), (F), (G), (I) and (K–N); SEM micrographs, (C), (E), (H) and (J). Anterior towards the left in (A–J, L) and towards the right in (K), (M) and (N). Abbreviations: gb, globular dentine; lb, lamellar bone; red dotted lines, contact surfaces between primary and secondary odontodes; white

dotted lines, border between globular dentine and basal bone; white dashed line, contact surfaces between primary odontodes in *Rongolepis*. Asterisks mark bone layers with fibre orientation parallel to the section axis. Scale bar equals 400 μm in (A), 100 μm in (B, G, H, M), 20 μm in (C), 200 μm in (D, F, K, N), 50 μm in (E, J, L), and 300 μm in (I).

7
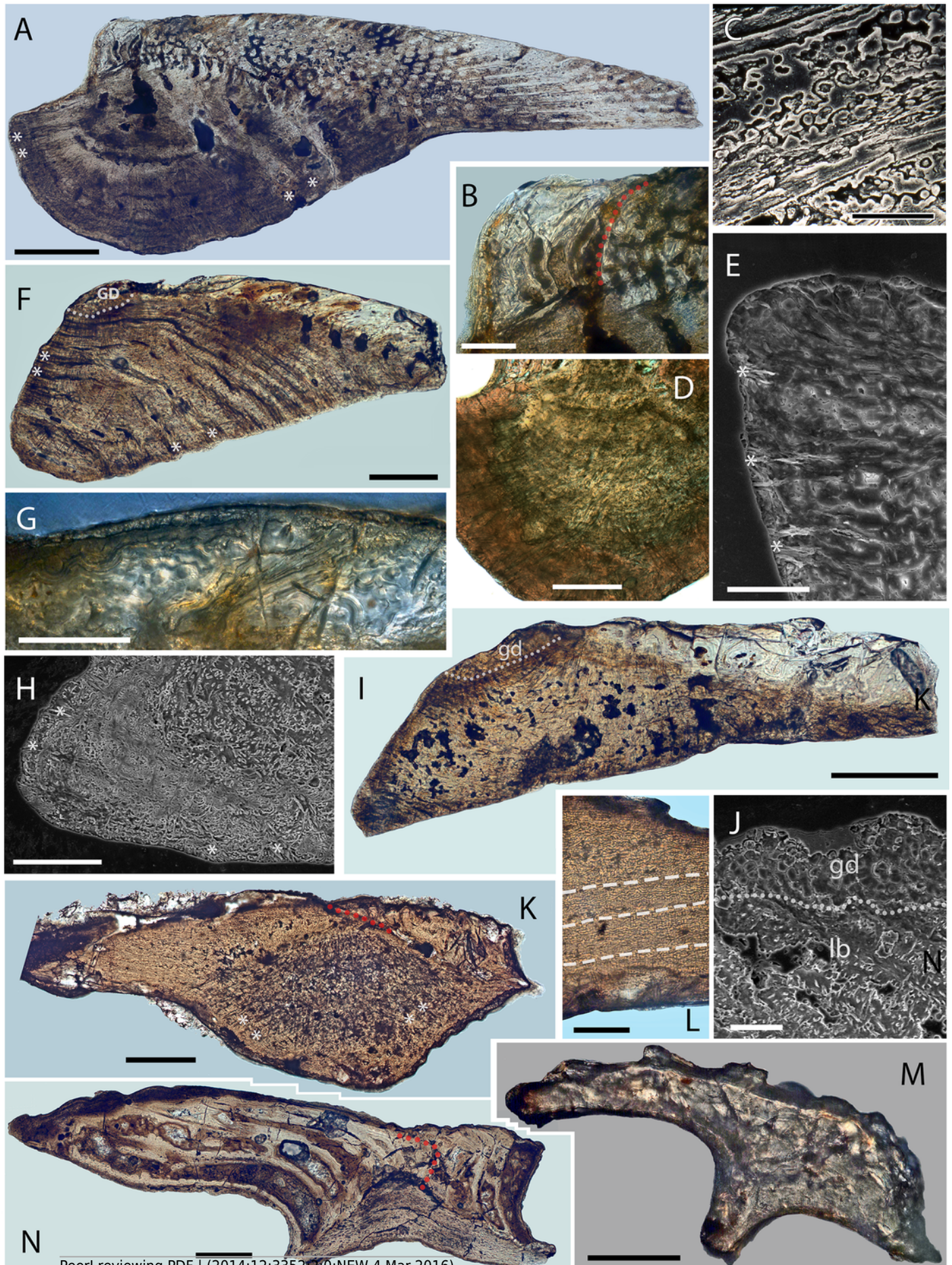
Histology of *Solinalepis levis* gen. et sp. nov. scales

Figure 7 **Histology of *Solinalepis levis* gen. et sp. nov. scales.** (A) thin-sectioned head scale (BU5317) from the Harding Sandstone, Colorado, USA; (B) transverse section of a *Solinalepis levis* gen. et sp. nov. trunk scale (BU5316) from the Harding Sandstone, Colorado, USA. Scale bar equals 200 µm in (A) and 100 µm in (B).

8
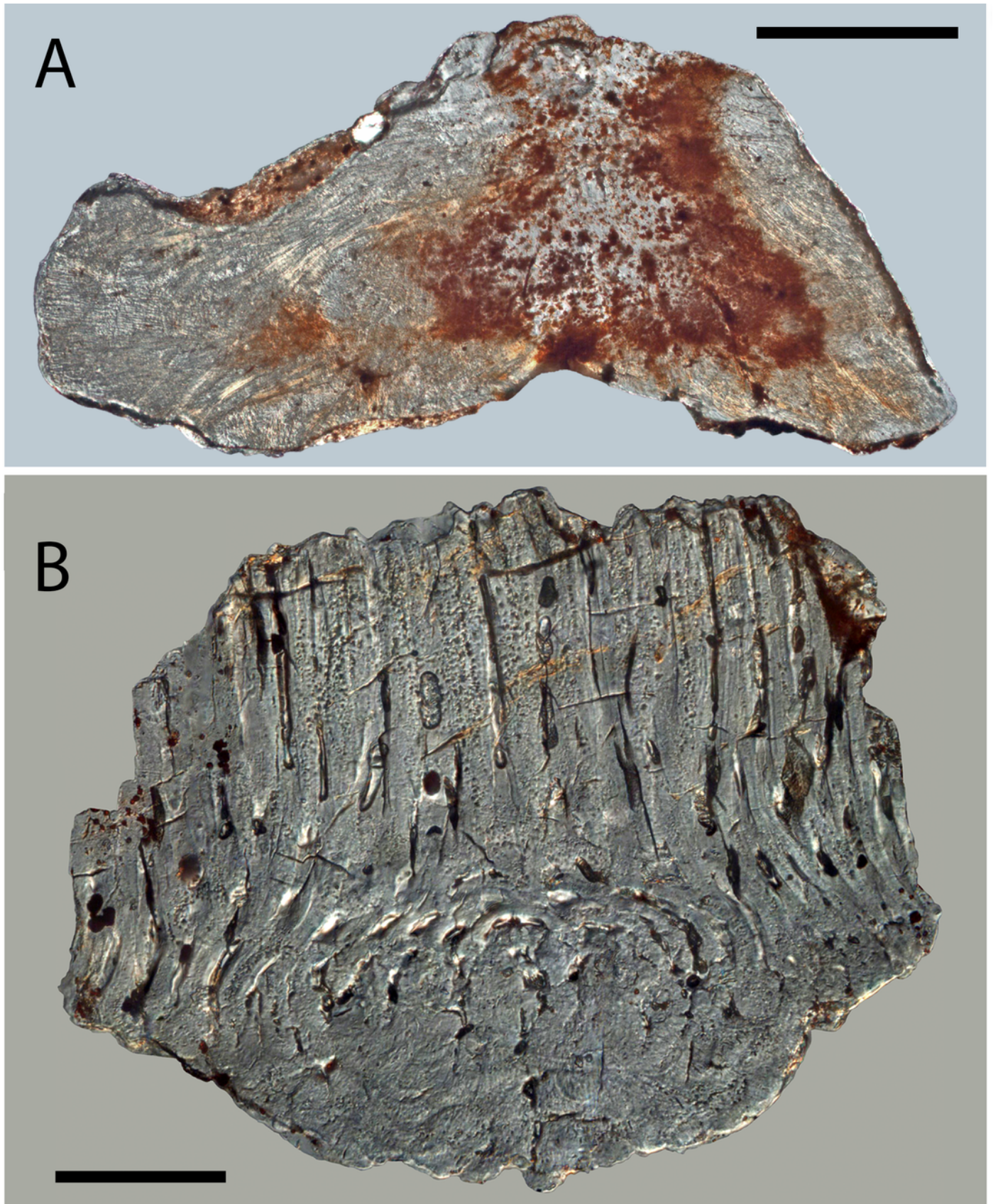
Canal system of mongolepid scales

Figure 8 **Canal system of mongolepid scales.** Volume renderings. (A–C) canals (red) inside a translucent *Mongolepis rozmanae* scale (BU5296) in (A) lateral view, in (B) posterior view sliced along the plane 1 and in (C, C1) crown view sliced along plane 2; (D, D1) canals in a transversely sliced *Teslepis jucunda* scale (BU5325) shown in posterior view; (E) pulp cavities (red) in a transversely sliced *Sodolepis lucens* scale (BU5305) shown in postero-lateral view; (F) longitudinally sliced *Shiqianolepis hollandi* scale (NIGP 130307) in baso-lateral view; (G, H) longitudinally sliced *Xinjiangichthys pluridentatus* scale IVPP V X2 in (G) posterior and (H) lateral views; (I, J) canals system (red) inside a transversely sliced *Solinalepis levis* gen. et sp. nov. scale (BU5318) shown in posterior view, (J) detail of (I). Horizontal canals depicted in purple in c1 and d1. Yellow arrowheads point at canal openings on the sub-crown surface. Red dotted line, contact surfaces between primary and secondary odontodes; grey dotted line, crown/base border. Scale bar equals 400 µm in (A–C), 100 µm in (D, H, I), 200 µm in (E), 300 µm (F, G) and 50 µm in (J).
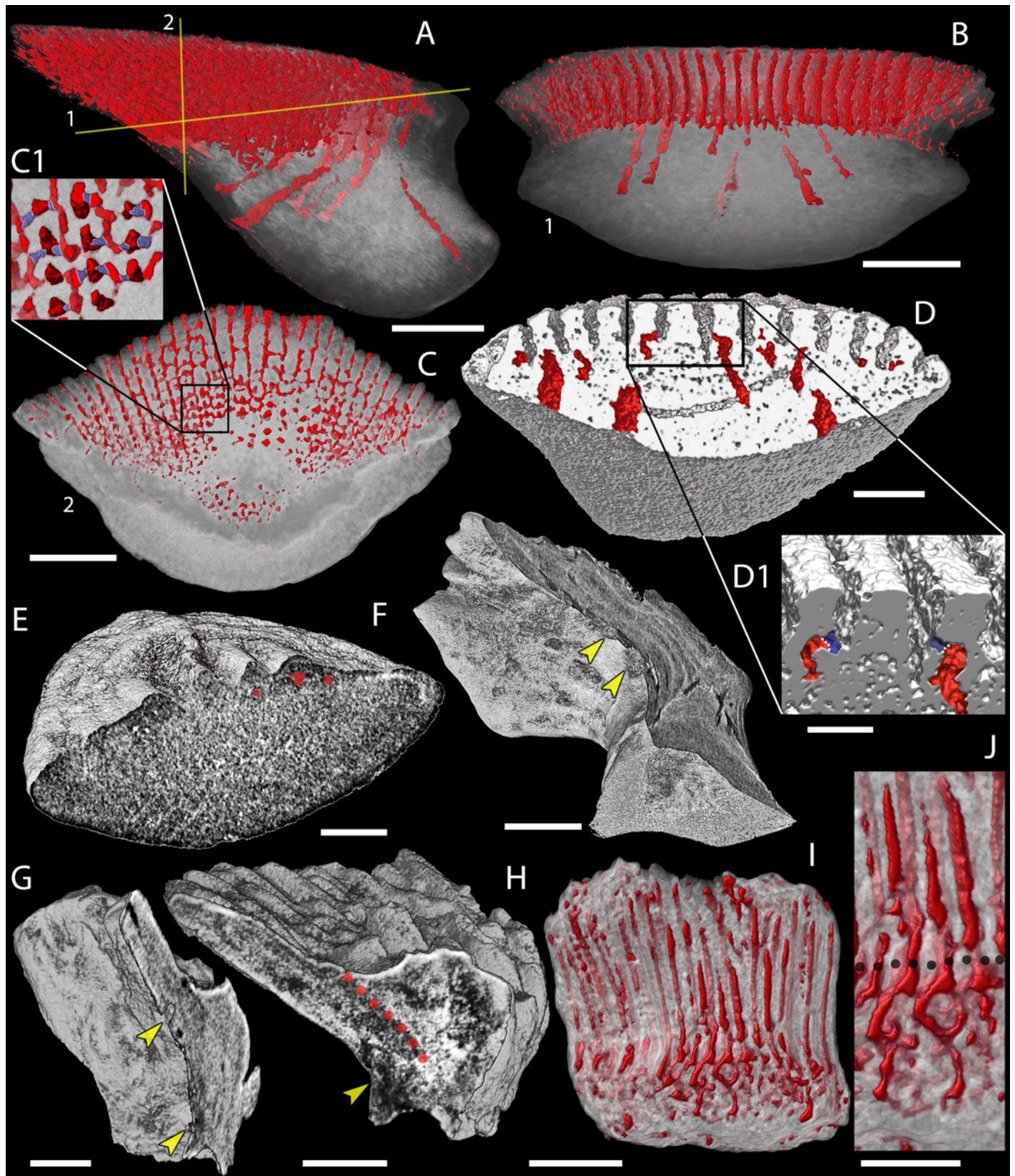
Odontocomplex organization of mongolepid scale crowns

Figure 9 **Odontocomplex organization of mongolepid scale crowns.** (A) *Teslepis jucunda* (BU5323) scale, medial portion of the crown; (B) *Shiqianolepis hollandi* (NIGP 130309) scale, medial portion of the crown; (C) *Solinalepis levis* gen. et sp. nov. trunk scale (BU5314), lateral portion of the crown. Primary odontocomplex structure in Mongolepidida demonstrated by line drawings of longitudinally sectioned (D) *Mongolepis rozmanae* (BU5297) and (E) *Shiqianolepis hollandi* (NIGP 130312) scales. In (A–C) some of the odontocomplexes are highlighted in red and green. Dark green and dark red, odd numbered odontodes; light green and light red, even numbered odontodes. In (D, E)—light grey, primary odontodes; light yellow, secondary odontodes. Anterior towards the bottom in (A–C) and towards the left in (D, E). Scale bar equals 100 µm in (A), 200 µm in (B) and 50 µm in (C).